

Programmed Cell Death Occurs Asymmetrically during Abscission in Tomato

Tal Bar-Dror,^{a,b} Marina Dermastia,^c Aleš Kladičnik,^d Magda Tušek Žnidarič,^c Maruša Pompe Novak,^c Shimon Meir,^a Shaul Burd,^a Sonia Philosoph-Hadas,^a Naomi Ori,^b Lilian Sonogo,^a Martin B. Dickman,^e and Amnon Lers^{a,1}

^aDepartment of Postharvest Science of Fresh Produce, Agricultural Research Organization, The Volcani Center, Bet Dagan 50250, Israel

^bThe Robert H. Smith Institute of Plant Sciences and Genetics in Agriculture, The Robert H. Smith Faculty of Agriculture, Food, and Environment, The Hebrew University of Jerusalem, Rehovot 76100, Israel

^cDepartment of Biotechnology and Systems Biology, National Institute of Biology, SI-1000 Ljubljana, Slovenia

^dDepartment of Biology, Biotechnical Faculty, University of Ljubljana, SI-1000 Ljubljana, Slovenia

^eDepartment of Plant Pathology and Microbiology, Institute for Plant Genomics and Biotechnology, Texas A&M University, College Station, Texas 77843

Abscission occurs specifically in the abscission zone (AZ) tissue as a natural stage of plant development. Previously, we observed delay of tomato (*Solanum lycopersicum*) leaf abscission when the LX ribonuclease (LX) was inhibited. The known association between LX expression and programmed cell death (PCD) suggested involvement of PCD in abscission. In this study, hallmarks of PCD were identified in the tomato leaf and flower AZs during the late stage of abscission. These included loss of cell viability, altered nuclear morphology, DNA fragmentation, elevated levels of reactive oxygen species and enzymatic activities, and expression of PCD-associated genes. Overexpression of antiapoptotic proteins resulted in retarded abscission, indicating PCD requirement. PCD, LX, and nuclease gene expression were visualized primarily in the AZ distal tissue, demonstrating an asymmetry between the two AZ sides. Asymmetric expression was observed for genes associated with cell wall hydrolysis, leading to AZ, or associated with ethylene biosynthesis, which induces abscission. These results suggest that different abscission-related processes occur asymmetrically between the AZ proximal and distal sides. Taken together, our findings identify PCD as a key mechanism that occurs asymmetrically during normal progression of abscission and suggest an important role for LX in this PCD process.

INTRODUCTION

Abscission is a highly temporally and spatially regulated process in which various organs, including leaves, flowers, and flower organs or fruits are separated from the mother plant (Roberts et al., 2002; Leslie et al., 2007). The basis for organ abscission is considered to be a cell separation process, which occurs specifically in the preformed abscission zone (AZ) tissue located at the base of the organ to be shed. The AZ is morphologically and physiologically distinct from neighboring cells and includes smaller-sized, cytoplasmically dense cells forming from one to ~50 cell layers in different plants (Osborne and Sargent, 1976; Roberts et al., 1984; Leslie et al., 2007; van Nocker, 2009).

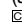
Based on anatomical, physiological, genetic, and molecular studies, the abscission process requires four successive phases

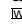
for its successful execution (Roberts et al., 2000; Patterson, 2001; Taylor and Whitelaw, 2001; Jarvis et al., 2003; Leslie et al., 2007). The first phase involves early differentiation of cells localized at the site of the future organ separation into a determined AZ. In the second phase, the differentiated AZ acquires competence to respond to the abscission signal(s), presumably via developmental and hormonal cues. The third phase is an ethylene-mediated execution of abscission via a cell separation process, which involves a major induction of cell wall-modifying and hydrolytic enzymes, causing degradation of the middle lamella between AZ cells to allow physical separation of the abscised organ from the mother plant. The last phase, which overlaps with stage three and follows detachment, includes the development of a protective layer at the surface of the exposed tissue, creating a scar at the site of organ detachment on the plant body.

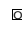
In recent years, progress has been made in the study of several phases of the abscission process largely in *Arabidopsis thaliana*, tomato (*Solanum lycopersicum*), and citrus model systems. Several proteins have been shown to have a regulatory role in abscission, including potential signal molecules and receptors (Lewis et al., 2006; Cho et al., 2008; McKim et al., 2008; Stenvik et al., 2008; Liljegren et al., 2009; van Nocker, 2009). Transcriptomic analyses during abscission have identified genes that are regulated during this process (Cai and Lashbrook, 2008; Agustí et al., 2009; Meir et al., 2010).

¹ Address correspondence to alers@volcani.agri.gov.il.

The author responsible for distribution of materials integral to the findings presented in this article in accordance with the policy described in the Instructions for Authors (www.plantcell.org) is: Amnon Lers (alers@volcani.agri.gov.il).

 Some figures in this article are displayed in color online but in black and white in the print edition.

 Online version contains Web-only data.

 Open Access articles can be viewed online without a subscription. www.plantcell.org/cgi/doi/10.1105/tpc.111.092494

The AZ acquires competence to respond to ethylene, known to induce or accelerate abscission (Taylor and Whitelaw, 2001; Binder and Patterson, 2009). In many cases, the abscission process is induced by ethylene, while the rate and degree of abscission depends upon the endogenous balance between auxin and ethylene levels in the tissue (Patterson, 2001; Taylor and Whitelaw, 2001; Roberts et al., 2002; Meir et al., 2006, 2010): Auxin concentrations must be reduced in the AZ to render it sensitive to ethylene, which promotes the advancement of abscission (Abeles and Rubinstein, 1964; Sexton and Roberts, 1982). Based on expression patterns and modulation in transgenic plants and mutants, genes encoding polygalacturonases (PGs) and β -1,4-glucanases (cellulases) have been suggested to play a central role in the execution of cell separation (Greenberg et al., 1975; Lashbrook et al., 1998; Brummell et al., 1999; Hong et al., 2000; González-Carranza et al., 2007; Jiang et al., 2008; Ogawa et al., 2009). Other proteins associated with the AZ are expansin (Cho and Cosgrove, 2000; Belfield et al., 2005), pathogenesis-related proteins (Eyal et al., 1993; Coupe et al., 1997), and metallothioneins (Coupe et al., 1995), but their role in the process is not yet clear.

We previously showed that inhibiting expression of the ribonuclease gene *LX* results in retardation of leaf abscission in tomato (Lers et al., 2006). Tomato *LX* ribonuclease (*LX*) is a T2/S-like ribonuclease whose expression is known to be associated with phosphate starvation, ethylene responses, senescence, and programmed cell death (PCD) (Lers et al., 1998; Lehmann et al., 2001; Köck et al., 2006). Specific induction of the *LX* protein was detected around the mature tomato's AZ tissue. In a parallel study, we found that gene expression of the *Arabidopsis* nuclease *BFN1* is associated with PCD and is induced in the AZ. The AZ-specific expression of *BFN1* promoter was found to be conserved in both tomato leaf and flower/fruit AZs (Farage-Barhom et al., 2008). Based on these observations, we hypothesized that PCD is involved in abscission and is required for its normal progression and that *LX* has an important functional role in this PCD.

The results of the experiments described in this report provide considerable evidence for the occurrence and importance of PCD during the late stage of abscission and for its requirement for normal progression of the process. We further show that this PCD process occurs asymmetrically (i.e., only on the distal side of the fracture plane), indicating that differential abscission-related processes occur on the proximal and distal sides of the AZ. We propose that this spatial asymmetry is of functional significance for the abscission process.

RESULTS

Flower Abscission Is Delayed in *LX*-Inhibited Plants

We previously documented significant inhibition of tomato leaf abscission in *LX*-deficient transgenic plants (Lers et al., 2006). We examined whether or not flower abscission is also suppressed in three independent *LX*-inhibited tomato lines. Abscission was induced by removing flowers, and pedicel abscission was recorded. A marked difference was measured 24 h after

induction of flower pedicel abscission (Figure 1A). About 85% of the total pedicels had abscised in the wild type, in comparison to 47, 26, and 53%, respectively, in the transgenic lines H9, T2, and A2. *LX* protein levels measured in the flower AZ, 5 h after induction of abscission, confirmed lower *LX* expression in the transgenic plants (Figure 1B) but do not necessarily represent fully the levels of *LX* protein in the AZ of flower pedicels scored for abscission.

The plant hormones ethylene and auxin play central roles in regulating tomato organ abscission by inducing and inhibiting it, respectively. We had previously shown that ethylene induces *LX* expression at both the RNA and protein levels in the leaf (Lers et al., 1998, 2006). We tested whether the expression of the *LX* gene is accordingly regulated by these hormones using microarray analysis (Meir et al., 2010). AZ-specific expression of *LX* was activated following induction of pedicel abscission by flower removal, and this activation was nullified by either pretreatment with the ethylene action inhibitor 1-methylcyclopropene (1-MCP) or by application of the auxin indole-3-acetic acid (IAA) to the tomato pedicel following flower removal (Figure 2). Auxin also nullified the ethylene-induced expression of the *LX* protein in the leaf tissue (see Supplemental Figure 1 online). When external

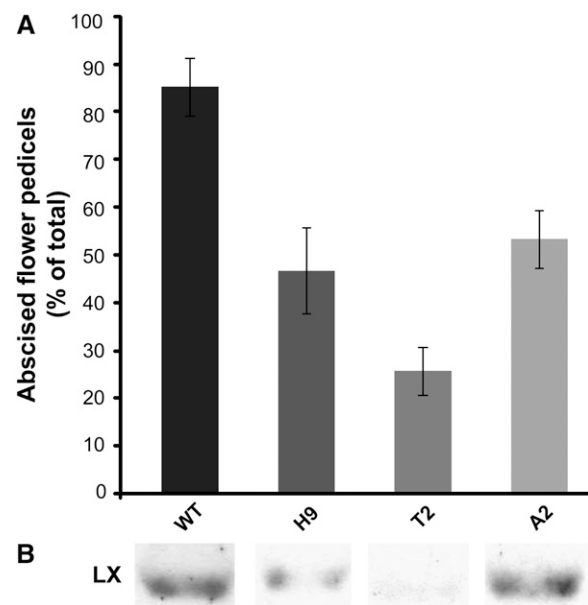


Figure 1. Abscission of Flower Pedicels Is Delayed in *LX*-Inhibited Transgenic Tomato Plants.

Abscission of flower pedicels was induced in the wild type (WT) (VF36) and three independent *LX*-inhibited tomato lines (H9, T2, and A2) by flower removal.

(A) The accumulated number of abscising pedicels after 24 h was recorded, and the percentages of abscising pedicels are presented. Four biologically independent treatments were performed in each one of the plant lines, and the total number of pedicels scored was 40 to 60. Error bars correspond to \pm SE.

(B) Level of the *LX* protein in AZ-containing tissue collected from the different plants 5 h after induction of abscission. *LX* level was measured following protein extraction by immunoblot analysis.

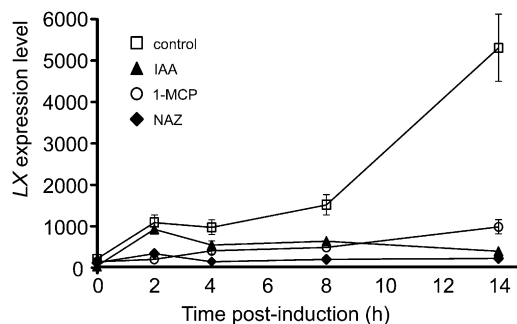


Figure 2. Effects of Flower Removal for Induction of Pedicel Abscission, 1-MCP Pretreatment, and IAA Application after Flower Removal on the Kinetics of Changes in Array-Measured LX Expression Levels during Tomato Pedicel Abscission.

ethylene was applied continuously to pedicels following induction of abscission, LX protein level in the AZ was not further induced, suggesting that the endogenous ethylene level is sufficient (see Supplemental Figure 2 online). External ethylene was also examined for effects on the rate of pedicel abscission in the LX-suppressed lines and was found to only partially relieve the inhibitory effect on abscission brought about by LX suppression (see Supplemental Figure 3 online).

LX Protein Is Localized on the Distal Side of the Leaf and Flower AZ Fractures

The LX protein was previously observed to be induced around the AZ tissue following induction of abscission (Lers et al., 2006). To more precisely localize the site of LX accumulation, an immunolocalization analysis was performed on AZ-containing sections sampled at the late stage of abscission, when separation had already initiated. Interestingly, LX was detected only on the distal side of the AZ fracture or on the distal side of the AZ where separation would occur (Figures 3A and 3B). Control preimmune serum showed no signal in adjacent tissue sections (Figure 3C).

This observation was further verified using immunoblot analysis. Pedicel abscission was induced in tomato flowers and 1- to 2-mm-thick tissue slices were collected separately from either side of the AZ tissue and used for immunoblot analysis. LX was detected mainly in the tissue localized on the distal side of the flower AZ relative to its low level on the proximal side, while in the nearby control tissue (non-AZ [NAZ]), almost no LX was detected (Figure 3D). Induction of the LX transcript, assayed by quantitative RT-PCR, was also observed mainly in the tissue distal to the AZ in both flower and leaf AZs (Figures 3E and 3F).

Loss of Cell Viability in the AZ prior to Leaf and Flower Abscission

To test the hypothesis that PCD is involved in tomato organ abscission, we first examined the incidence of death in cells of mature AZs, before the actual separation, using viability staining with Evans Blue (EB), a dye that is readily taken up specifically by

dead cells. Positive staining was clearly observed in cells in or near the tomato leaf AZ, in which the cell separation stage of abscission was initiated (see Supplemental Figures 4A to 4C online). In some cases, EB-positive staining was observed when the initial site of the abscission fracture was visible. This was observed not only on the internal tissue but also on the external side of the halved joint tissue (see Supplemental Figures 4D and 4E online). Similarly, EB staining was observed in the AZs of tree tobacco (*Nicotiana glauca*) leaves during abscission and at the site of flower organ shedding in *Arabidopsis* (see Supplemental Figures 4F to 4H online).

Changes in Cellular and Nuclear Morphology and DNA Fragmentation Support the Occurrence of PCD during Leaf and Flower Abscission

PCD involves a change in nuclear morphology, chromatin condensation, and nuclear DNA fragmentation. We examined whether any or all of these PCD hallmarks are present in the AZ tissue during the late stage of the abscission process induced by flower or leaf blade removal. Nuclear morphology was examined by fluorescence microscopy following DNA staining with 4',6-diamidino-2-phenylindole (DAPI) in the AZs of tomato flowers and leaves. In both cases, clear changes were observed in the nuclear morphology in abscission-induced AZ cells or in cells located in the surrounding tissue (Figure 4). Relative to control tissues, nuclei around AZ tissues after abscission induction had a markedly irregular shape, indicating chromatin disorganization and condensation (Figures 4A to 4D).

Sections of leaf AZ tissue, in which petiole separation was already initiated, were subjected to the TUNEL (for terminal deoxynucleotidyl transferase dUTP nick end labeling) assay (Gavrieli et al., 1992) for detection of chromosomal DNA fragmentation. Nuclei showing positive fluorescence staining were located predominantly on the distal side of the AZ fracture plane in cells localized on the edge of the leaf petiole to be separated from the main plant body (Figure 4E). The strongest TUNEL signal was recorded in nuclei of cells located near the fracture opening fork and below it, where the fracture is yet to be formed. No similar TUNEL-positive reaction was detected in cells located at a distance from the AZ tissue (Figure 4E) or in AZ tissue sections in which the abscission process had not been induced (see Supplemental Figure 5A online). The presence of DNA-containing nuclei on both sides of the AZ fracture was confirmed by DAPI staining of the same tissue sections (Figure 4F; see Supplemental Figure 5B online). These results indicate the occurrence of apoptotic-like features in the distal side of the AZ, supporting the involvement of PCD in abscission.

PCD in plants shows characteristic cellular, structural, and morphological features (Vanyushin et al., 2004; Cacas, 2010; van Doorn et al., 2011). We examined the occurrence of such features around the distal side of the tomato leaf AZ in comparison to the proximal side using transmission electron microscopy at 0 to 48 h after the 24-h ethylene treatment (Figure 5; see Supplemental Table 1 online). Several ultrastructural changes were detected already at the 4-h time point (see Supplemental Figure 6 and Supplemental Table 1 online), but they were much more pronounced at 48 h (Figure 5). The changes were

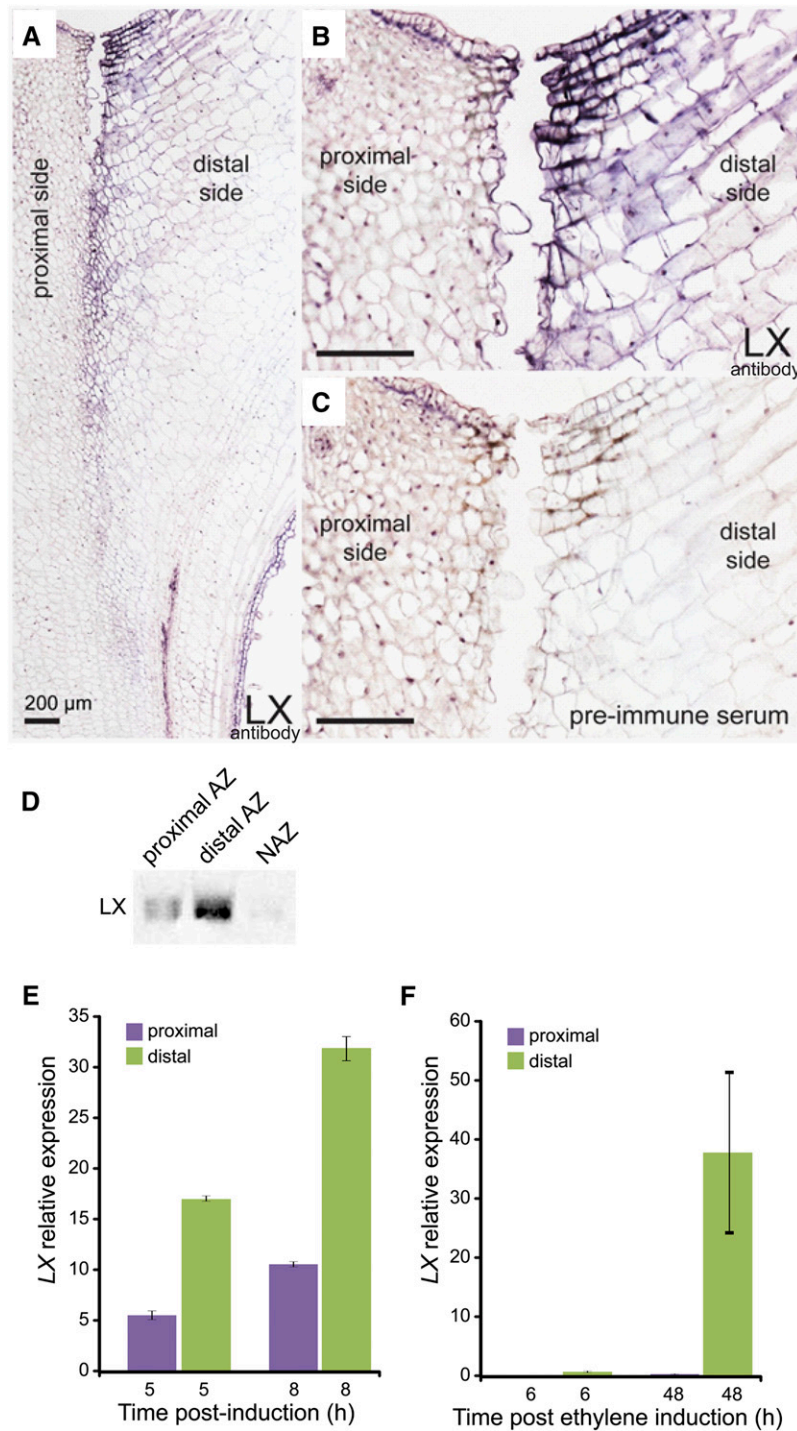


Figure 3. Immunolocalization of LX in Tomato Leaf Petiole AZ, Measurement of LX Level in the Flower Pedicel AZ and NAZ, and Measurement of LX Gene Expression Levels in Flower Pedicel and Leaf Petiole AZs.

Longitudinal sections of tomato leaf AZ during the cell separation stage (36 h after ethylene induction), including the stem and leaf petiole tissues, were subjected to immunolocalization of LX using an LX-specific antibody. Immunolocalization of LX in tomato leaf petiole AZ (**A**) to **C**], measurement of LX level in the flower pedicel AZ and NAZ (**D**), and measurement of LX gene expression levels in flower pedicel (**E**) and leaf petiole (**F**) AZs.

(A) Dark-purple staining indicates cells cross-reacting positively with the LX protein antibody; proximal and distal sides of the AZ fracture plane face the stem and leaf petiole, respectively.

(B) Magnification of the AZ tissue in which cell separation has already occurred, where only cells at the edge of the distal side are positively stained with

distributed gradually along the AZ fracture, according to its stage of separation, and differed between its proximal and distal sides (Figures 5B to 5K). While changes on the proximal side were limited to only two or three cell layers bordering the fracture, they were expressed throughout multiple layers on the distal side. Cells on the proximal side were densely cytoplasmic. Frequently, such cells showed amoeboid-shaped nuclei instead of the more usual rounded or oval ones, which were electron lucent (Figure 5D). The endomembrane system, composed of the endoplasmic reticulum (ER) and Golgi apparatus (Figures 5B, 5C, 5E, and 5G), was well developed. The hallmark of the proximal side of the AZ was expressed in extensive accumulation of vesicular structures (Figures 5E to 5G), including paramural bodies (PBs), in which small vesicles are located between the cell wall and the plasma membrane (Figures 5E and 5F). PBs were frequently associated with branched plasmodesmata that interconnected adjacent cells (Figure 5E) but were also found at other sites along the cell margin (Figure 5F). The numerous branched plasmodesmata had cavities (Figure 5F) (Burch-Smith et al., 2011), which could be markedly expanded (Figure 5C). At the late stage of abscission, the cells on the proximal side began to separate by gradual dissolution of the middle lamella. Cells that remained on the mother plant still maintained the highly developed endomembrane system (Figure 5G). On the distal side of the AZ fracture, cells exhibited different levels of degradation and changes that were followed by fracture development (Figures 5H to 5K). At the fracture front (Figure 5K), chloroplasts were densely packed with lipid-protein plastoglobuli, and their shape changed from oval to more round due to an increase in chloroplastic volume caused by luminal swelling compared with chloroplasts in cells at equivalent position in untreated plant (Figure 5A). The nuclei became electron dense and condensed (Figure 5J). In some cells, dilation of ER was observed (Figure 5I). Identification of dilated ER was unambiguous, as indicated by the presence of membrane-bound ribosomes (Figure 5I). Very early during the process in some cells, a detachment of plasma membrane from the cell wall was observed (Figures 5I and 5J; see Supplemental Figure 6 online). In the cytoplasm of some cells, small lytic vacuoles were formed (Figure 5J). On the distal side of the mature fracture, cells eventually died, and before dying, the cytoplasm appeared to be granulated. The tonoplast of the vacuole was ruptured and other endomembrane organelles were undergoing degradation. Because usually no clearing of the cytoplasm was observed, the corpses of dead cells remained largely unprocessed (Figure 5H). Overall, the observed changes in cellular structural and morphological features indicate clear differences between cells localized proximal or distal of the AZ. In cells localized on the distal side,

our observations are in line with the occurrence of PCD, but structural changes in cells localized on the proximal side are indicative of high metabolic activities.

Activation of Nuclease and Protease Activities and PCD-Associated Genes in the AZ

PCD has been associated with the induction of several nuclease and protease activities (Bozhkov and Jansson, 2007; Bonneau et al., 2008; Aleksandrushkina and Vanyushin, 2009; Woltering, 2010). Using an activity gel assay, a specific nuclease activity was observed specifically in the tomato flower AZ-containing tissue, only at late stages of abscission (Figure 6A). Similar induction of nuclease activity was visualized specifically in the petiole AZ tissue of tree tobacco following induction of leaf abscission (Figure 6A). Nuclease activity was detected mainly in the tissue located on the distal side of the flower AZ (Figure 6B), where LX protein accumulation (Figure 3D) and markers of PCD (Figure 4) had also been localized. This distal side-specific nuclease might be encoded by the tomato *TBN1* gene (Matousek et al., 2007), whose expression was also found by quantitative RT-PCR to be induced mainly on the distal side of the AZ (Figure 6C).

Abscission-associated proteolytic activity was also identified in the late stage of the abscission process in tomato leaf AZ (Figure 6D) but not in young petiole in which abscission is not induced (Figure 6D). Specific induction of a Cys and Ser, SBT3, protease-encoding genes was observed (Figures 6E and 6F) in a microarray analysis of the abscission-related transcriptome of tomato flower AZ (Meir et al., 2010). Pretreatment with the ethylene action inhibitor 1-MCP inhibited this expression, suggesting positive regulation by ethylene. The observed transient early induction of these genes may be a result from the ethylene produced in response to wounding due to flower removal.

Sphingosine-1-phosphate lyase (SPL) is associated with mammalian cell death signaling (Reiss et al., 2004; Oskouian et al., 2006), and in plants, it is induced during senescence and following induction of cell death (Reiss et al., 2004; Niu et al., 2007). The tomato *SPL* gene was induced in the AZ tissue at the late stage of abscission (see Supplemental Figure 7A online). The expression pattern of *pirin*, a PCD-related gene (Orzaez et al., 2001), showed a transient induction in the AZ following flower removal to induce abscission and a second increase in expression during the late stage of abscission (see Supplemental Figure 7B online). Levels of the *pirin* transcript were significantly higher on the distal side of the flower AZ (see Supplemental Figure 7C online). The late AZ-specific increase in the expression of *SPL* and *pirin* was inhibited by 1-MCP pretreatment.

Figure 3. (continued).

the LX antibody. Bar = 200 μm .

(C) Magnification of a sequential serial section of the AZ tissue, in which the immunolocalization assay was performed with preimmune serum showing no LX-specific staining. Bar = 200 μm .

(D) Immunoblot analysis using proteins extracted from tissue sampled separately from either the proximal or distal sides of the tomato flower pedicel AZ, and proteins extracted from nearby (a few millimeters away) stem tissue as a control (NAZ).

(E) and (F) RNA was extracted from either the proximal or distal sides of the AZ and used for quantitative real-time PCR analysis performed for flower (E) and leaf (F) AZ. Error bars correspond to $\pm\text{SD}$.

[See online article for color version of this figure.]

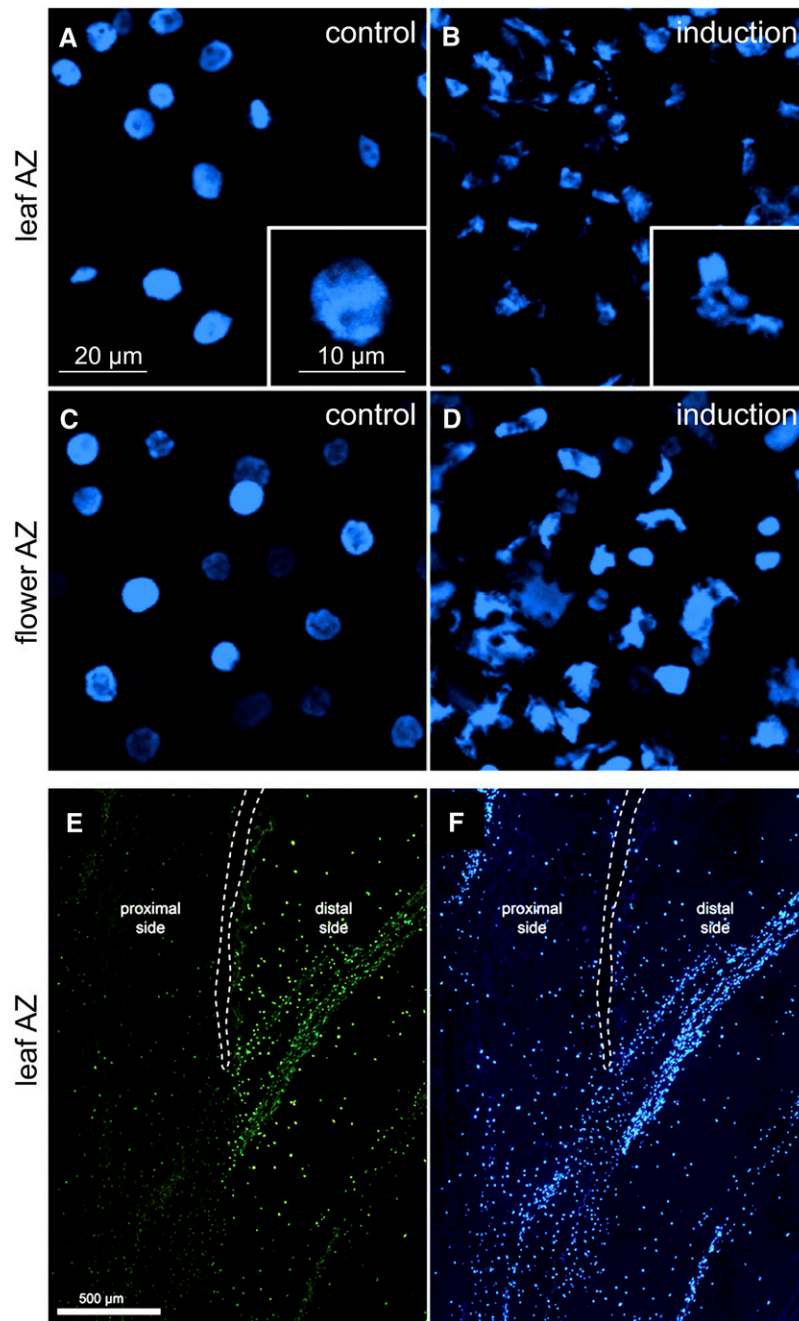


Figure 4. Changes in Nuclear Morphology in the Tomato Leaf and Flower AZs and Nuclear DNA Fragmentation in Cells on the Distal Side of the AZ.

For observing nuclear morphology, abscission was induced either by flower removal or leaf deblading followed by a 24-h exposure to ethylene, and the pedicel or petiole AZs were separated at the late stage of the process. The exposed AZ fracture plane surfaces were subjected to DAPI nuclear staining. **(A)** Representative images are shown of the fracture plane of the leaf AZ not induced for abscission, including a scaled-up image of one representative nucleus.

(B) Image of the leaf AZ at the late stage of induced abscission, including a scaled-up image of one representative nucleus.

(C) Image of the flower AZ not induced for abscission.

(D) Image of the flower AZ at the late stage of induced abscission.

(E) and **(F)** For detection of DNA fragmentation, a longitudinal section of tomato leaf AZ during the cell separation stage (24 h after ethylene treatment), including the stem and leaf petiole tissues, was stained by TUNEL-labeling assay **(E)** or by DAPI **(F)**. TUNEL-positive nuclei, characterized by bright-green fluorescence, are localized on the distal side of the leaf AZ (toward the leaf petiole). White dotted lines outline the fracture in the AZ formed due to cell separation.

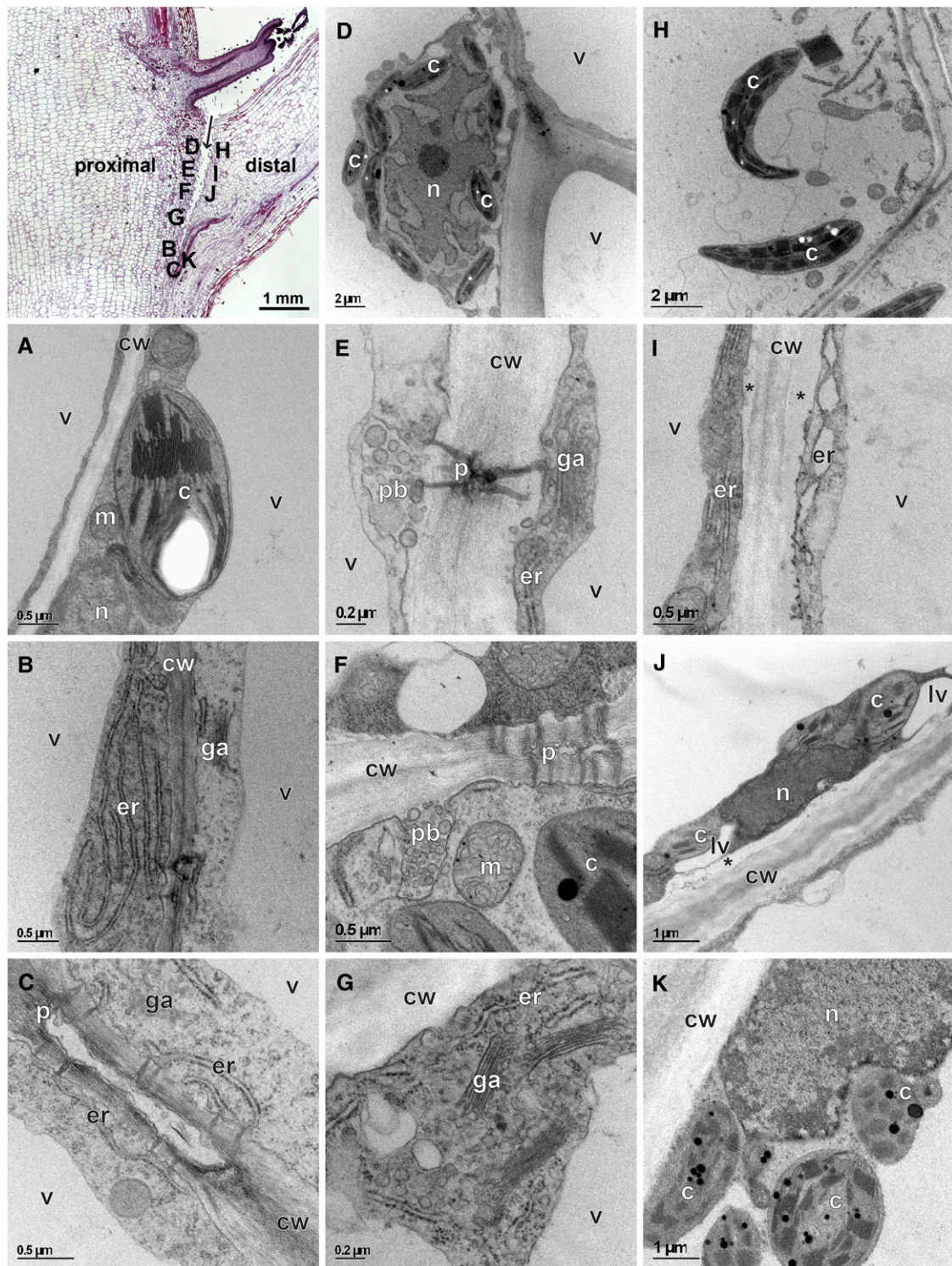


Figure 5. Transmission Electron Micrographs of Cells in Tomato Leaf AZ Showing Ultrastructural Changes 48 h after Induction of Abscission by Leaf Deblading and Ethylene Treatment.

The position of cells within the tissue is labeled on the light microscopy image in the top left corner (arrow marks the AZ fracture plane). Asterisks mark detachment of plasma membrane from the cell wall. Cell organelle labeling: c, chloroplast; cw, cell wall; er, endoplasmic reticulum; ga, Golgi apparatus; lv, lytic vacuole; m, mitochondria; n, nucleus; p, plasmodesmata; pb, paramural body; v, vacuole.

Reactive Oxygen Species and Activation of the NADPH Oxidase Gene Occur in the Flower AZ following Induction of Abscission

The involvement of reactive oxygen species (ROS) in PCD processes in plants has been demonstrated (Gadjev et al., 2008). To examine whether differences in ROS levels can be visualized near the AZ following induction of the abscission process, staining of flower AZ cross sections with the fluorescent ROS indicator dye 2',7'-dichlorofluorescein diacetate (DCF) was performed. An increase in the level of ROS was observed around the flower AZ following induction of abscission by flower removal (Figures 7A to 7D). The level of ROS accumulation was also examined in exposed cells on the surface of the distal or proximal sides of the AZ fracture: Staining with DCF was performed at the very late stage, around 10 to 14 h following abscission induction, at which time pedicel abscission is estimated to be executed (Meir et al., 2010). The two AZ sides of the pedicel were separated, and the exposed fracture planes were immediately stained with DCF. As a control, noninduced pedicel AZ tissue was subjected to forced separation, resulting in fracture at the expected site of separation in the AZ. A higher level of ROS was observed in cells on the surface of the exposed AZ fractures following induction of abscission (Figures 7F and 7H) compared with the control tissue in which abscission was not induced (Figures 7E and 7G). A significantly higher ROS staining was visualized on the distal AZ fracture plane (Figure 7H) compared with that observed on the proximal AZ surface (Figure 7F).

NADPH oxidase is involved in ROS production during plant stress responses (to biotic and abiotic stress) and during PCD (Torres et al., 2002; Torres and Dangl, 2005). Expression of the tomato NADPH oxidase gene *RBOH1* was measured in the flower AZ using quantitative RT-PCR analysis and was found to be specific to the AZ tissue and induced primarily in the late stage of abscission, 8 h after flower removal (Figure 7I).

Leaf and Flower Abscission Is Retarded in Transgenic Plants That Overexpress Antiapoptotic Proteins

If PCD is indeed involved in the abscission process, as hypothesized, we expect repression of abscission in plants expressing

genes that prevent PCD, such as the fall armyworm (*Spodoptera frugiperda*) inhibitor of apoptosis protein, Sf IAP. Members of the IAP family function as cell death suppressors in eukaryotes (Deveraux and Reed, 1999; Yang and Li, 2000). Two independent tomato transgenic lines, *IAP-1* and *IAP-3* (Li et al., 2010), were analyzed for their effect on the abscission process. A clear delay in abscission progression was measured in both *IAP*-overexpressing tomato lines in comparison to their respective wild-type controls (Figure 8). When petiole abscission was monitored following induction by leaf deblading and ethylene treatment, the delay in abscission was more pronounced, by up to 8 d following induction of abscission. At this time point, petiole abscission was delayed by >50% in the transgenic plants compared with the wild type (Figure 8A). In experiments comparing pedicel abscission rates between the overexpressing lines and their respective wild-type controls, a clear and reproducible delay of pedicel abscission was observed (Figure 8B).

Overexpression of an unrelated antiapoptotic protein was also examined for its effect on abscission: Overexpression of the *p35* gene has been reported to inhibit PCD in tomato (Lincoln et al., 2002). Advancement of pedicel abscission was monitored and compared between wild-type and *p35*-transgenic plants. This analysis revealed a clear retardation of pedicel abscission in the *p35*-transgenic line, which was ~50% lower than that in the respective tomato wild type (Figure 8C).

Abscission-Associated Genes Are Differentially Expressed on the Proximal and Distal Sides of the Flower AZ

We tested whether the asymmetry between the proximal and distal sides of the AZ also occurs in the expression of genes previously reported to be associated with abscission. The overall kinetics of expression of the two tomato abscission-related polygalacturonase (*TAPG*) genes, *TAPG1* and *TAPG4*, during pedicel abscission was very similar to that reported previously (Kalaitzis et al., 1997; Meir et al., 2010). However, they were also expressed at a significantly higher level in the proximal side of the AZ (Figures 9A and 9B), where PCD was not observed to occur (Figure 4). On the other hand, expression of the tomato cellulase (β -1,4-endoglucanase) gene *Cel1*, involved in cell wall metabolism, and of the 1-aminocyclopropane-1-carboxylic acid synthase gene

Figure 5. (continued).

- (A) Intact control taken from the middle of the AZ in untreated plant.
- (B) to (G) Proximal side of the leaf treated with ethylene.
- (B) Extensive portion of the ER.
- (C) Branched plasmodesmata with enlarged cavity connected to ER on both sides of the cell wall.
- (D) Ameboidal nucleus.
- (E) Branched plasmodesmata connected to the PB.
- (F) Branched plasmodesmata with cavities that are not connected to the PB.
- (G) Cells on the proximal side after releasing the petiole, with retained extensive membrane and vesicular portion.
- (H) to (J) Distal side of the leaf treated with ethylene.
- (H) Shrunken chloroplasts and disintegrated cytoplasm.
- (I) Dilated ER.
- (J) Condensed nucleus.
- (K) Cells at the fracture front with swollen chloroplasts containing plastoglobuli.

[See online article for color version of this figure.]

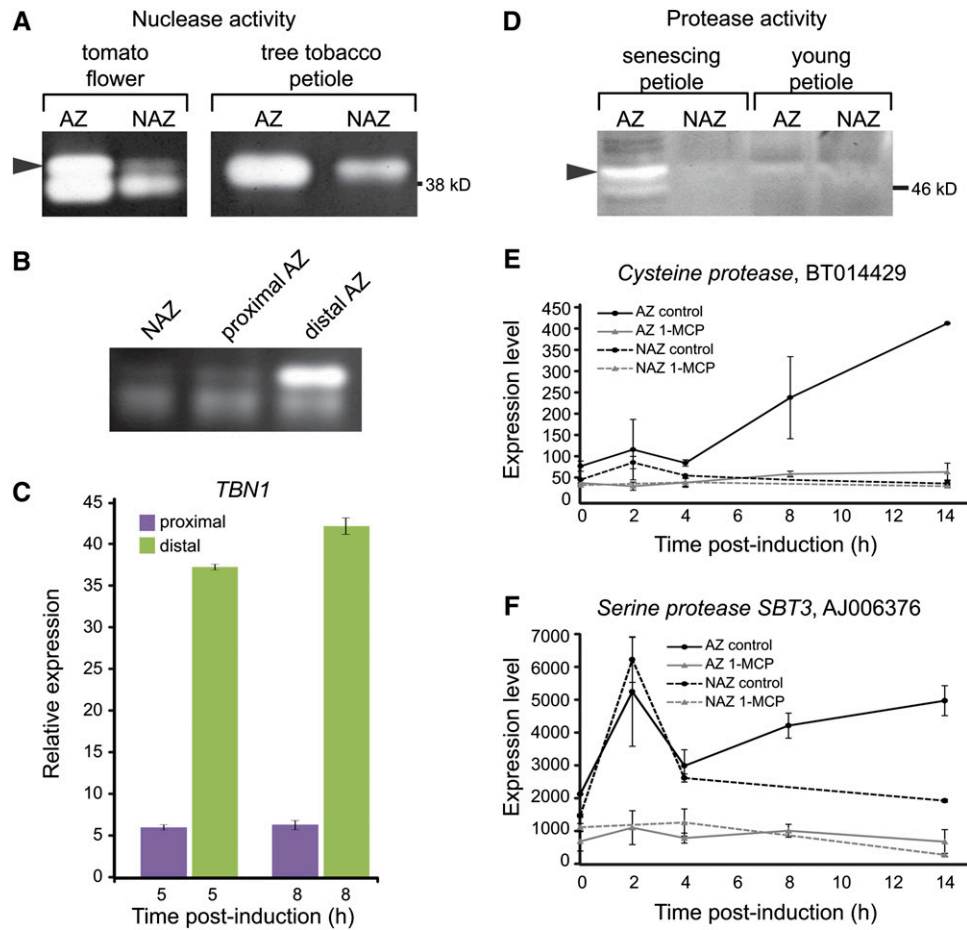


Figure 6. Nuclease and Protease Activities and Their Encoding Genes Are Induced in the AZ following Induction of Flower and Leaf Abscission.

(A) Nuclease activity induced in the tomato flower pedicel and tree tobacco leaf petiole AZs. Total proteins (5 μ g) extracted from AZ tissue or nearby NAZ tissue as a control were subjected to nuclease activity gel assay. Arrowhead marks position of the AZ-induced nuclease activity.

(B) Nuclease activity induced on the distal side of the tomato flower pedicel AZ. Proteins (5 μ g) extracted from either the AZ proximal or distal tissue were used for the nuclease activity gel assay.

(C) Quantitative real-time PCR analysis for the nuclease gene *TBN1* performed with RNA extracted from tomato tissues sampled from either the proximal or distal sides of the AZ at the indicated times following induction of pedicel abscission by flower removal.

(D) Protease activity induced in tomato leaf AZ. Proteins (10 μ g), extracted from the AZ or NAZ tissues of mature leaf petiole approaching abscission and young leaf petiole were subjected to protease activity gel assay. Arrowhead marks position of the AZ-induced protease activity.

(E) and **(F)** Microarray analysis results are shown for genes encoding Cys protease **(E)** and Ser protease **(F)** in the AZ and NAZ tissues, with or without 1-MCP pretreatment. The results demonstrate induction of expression mainly in the tomato flower pedicel AZ following induction of the pedicel abscission process by flower removal. Error bars correspond to \pm SD.

[See online article for color version of this figure.]

ACS (*TOMACS*), involved in ethylene biosynthesis, was found to be significantly higher on the distal side of the AZ (Figures 9C and 9D).

DISCUSSION

PCD Hallmarks Are Evident in the Late Stages of Abscission in Cells on the Distal Side of the AZ

Based on the association between *LX* expression and PCD processes (Lers et al., 1998; Lehmann et al., 2001), we raised the

hypothesis that during abscission, PCD, involving *LX*, occurs and is required for normal progression of abscission (Lers et al., 2006). Previous observations in a variety of plants, including *Prunus persica*, *Chamaelucium uncinatum*, *Pelargonium* \times *Hortorum*, and *Diospyros kaki*, support the hypothesis that cells immediately adjacent to the AZ might lose viability (Evensen et al., 1993; Tirlapur et al., 1995; van Doorn and Stead, 1997; Roberts, 2000; Kitajima et al., 2003; Macnish et al., 2005). We demonstrated the occurrence of PCD by the identification of several hallmarks of the process. Interestingly, nuclear morphology changes (Figure 4), as well as the induction of the *LX* protein (Figure 3D) and

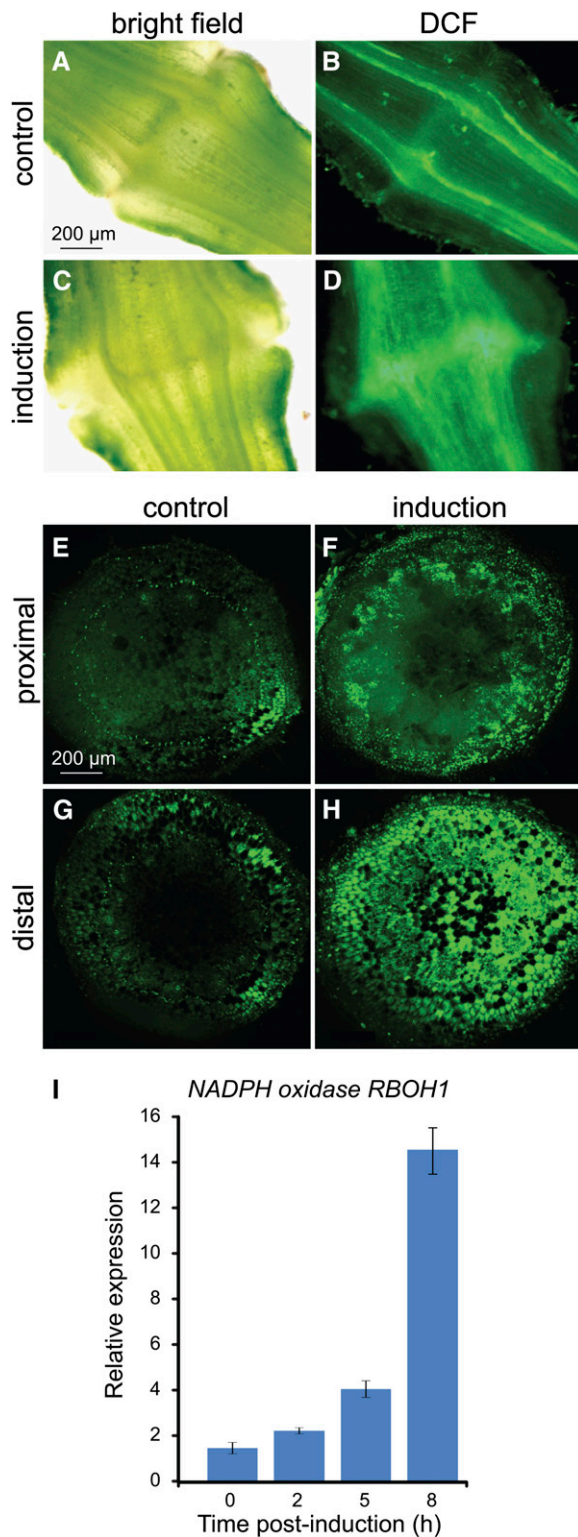


Figure 7. ROS Levels and NADPH Oxidase Gene Expression Are Induced in the Tomato Flower AZ following Induction of Pedicel Abscission by Flower Removal.

(A) to (H) ROS staining with DCF was performed on AZ cross sections in

nuclease activity (Figure 6B), were only visualized in cell layers on the distal side of the AZ, indicating that PCD is localized and restricted to the edge of the leaf petiole or flower pedicel. Clear evidence of different processes occurring on the distal and proximal sides of the leaf AZ was also visualized by transmission electron microscopy analysis, which revealed several markers generally associated with cell disruption and cell death only on the distal side of the AZ fracture (Figure 5).

Based on the observed ultrastructural changes (Figures 5H to 5K; see Supplemental Table 1 online), the type of PCD that occurs in the AZ cannot be confidently predicted (van Doorn et al., 2011). Several features of vacuolar PCD (e.g., formation of small lytic vacuoles and rupture of the tonoplast) were recorded; by contrast, the process was relatively fast and cell corpses remained largely unprocessed, which are characteristics of necrotic PCD (van Doorn et al., 2011). Although detachment of plasma membrane from the cell wall, a typical sign of necrosis (van Doorn et al., 2011), was observed in some AZ dying cells, usually the plasma membranes did not rupture; accordingly, there was no shrinkage of the protoplast. Several PCD morphologies and regulatory genes overlap and are observed, for example, in both apoptosis and autophagy, thus further complicating matters.

In addition, some features that are not typical of plant PCD were detected. Among them, the widening of the ER lumen was notable (Figure 5I): This phenomenon has been reported in virus-infected *Thlaspi arvense* (Hoefert, 1975) and in response to accumulation of misfolded proteins in *Phaseolus lunatus* cells (Sparvoli et al., 2000). The accumulation of type IV collagen in dilated ER leads to apoptosis in Hsp47-knockout mouse embryos via induction of CHOP (Marutani et al., 2004), and dilated ER has been suggested to enhance the misfolding of pro-insulin molecules (Despa, 2009). The precise role of the dilated ER during abscission is currently unknown. An additional interesting observation was that chloroplasts located distal to the point of fracture initiation were swollen with numerous plastoglobuli, as has been reported for senescing chloroplasts (Guiamet et al., 1999; Ghosh et al., 2001).

Induction of different nuclease and protease activities has been associated with the occurrence of PCD (Ito and Fukuda, 2002; Lam, 2008; Aleksandrushkina and Vanyushin, 2009; Reape and McCabe, 2010; Woltering, 2010). Our observations, including those reported here (Figure 6) and the previously described activation of the promoter of the *BFN1* nuclease gene in abscission (Farage-Barhom et al., 2008), indicate involvement

control flower AZ not induced for abscission (B) and ~10 h after induction of pedicel abscission by flower removal (D). Bright-field images of the same control (A) and abscission-induced (C) tissue sections. ROS detection was performed also in the exposed AZ surface separating the proximal and distal sides, and fluorescent images of the fracture planes were taken. Representative images of the proximal (E) and distal (G) sides of the pedicel AZ not induced for abscission and of the proximal (F) and distal (H) side of the pedicel AZ induced for abscission are shown. (I) Quantitative real-time PCR expression analysis of the tomato *NADPH oxidase* gene in the flower AZ during pedicel abscission. Error bars correspond to \pm SD.

[See online article for color version of this figure.]

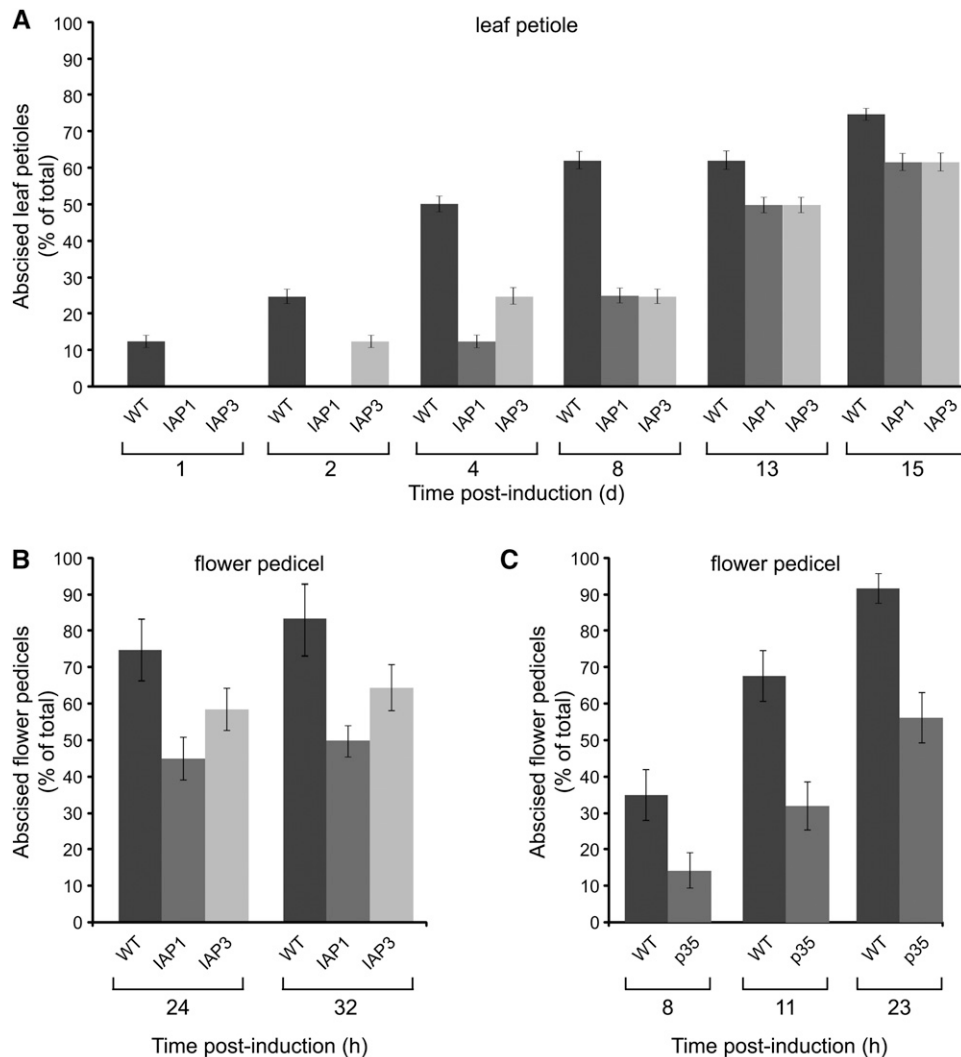


Figure 8. Organ Abscission Is Delayed in Tomato Transgenic Plants Overexpressing an IAP.

Leaf petiole (**A**) and flower pedicel (**B**) abscission in two independent transgenic plants overexpressing the *IAP* gene compared with that measured in the respective Rutgers wild type (WT). Flower pedicel abscission in plants overexpressing the *P35 IAP* gene compared with that measured in the respective asc wild type (**C**). Leaf abscission experiments were performed with plants developing six to eight leaves. Petiole abscission of the first leaf was induced by leaf deblading, followed by exposure to ethylene for 24 h. Pedicel abscission was induced by flower removal. Error bars correspond to \pm SD.

of nucleases and proteases with abscission possibly having a role in the documented PCD. Furthermore, protease-encoding genes were previously shown to be induced in AZs during abscission in other plants (Helm et al., 2008; Tripathi et al., 2009), including induction of a PCD-associated metacaspase gene (Castillo-Olamendi et al., 2007).

ROS are key components in plant PCD associated with developmental processes and environmental stress responses (Van Breusegem and Dat, 2006; Gadjev et al., 2008). NADPH oxidase has been established as a key enzyme for ROS production in plants' responses to biotic and abiotic stresses and during PCD (Torres et al., 2002; Torres and Dangl, 2005). Our results indicate involvement of both ROS accumulation and *NADPH oxidase* gene induction in the AZ PCD (Figure 7). Hydrogen peroxide (H_2O_2) was

previously shown to be involved in in vitro-induced abscission in *Capsicum* (Sakamoto et al., 2008). Application of ROS scavengers or an inhibitor of NADPH oxidase resulted in delayed abscission (Sakamoto et al., 2008). Several studies have shown induction during abscission of antioxidative components (Henry et al., 1974; Wang et al., 2005; Meir et al., 2006, 2010; Cai and Lashbrook, 2008); however, its causal relationship with the observed ROS induction in the AZ awaits clarification.

While PCD is clearly associated with abscission, further research is required to establish the relationship between the observed PCD and the underlying regulatory mechanisms and execution of abscission. A possible link could be ethylene, which is known to have a significant regulatory role for both abscission and PCD (Roberts et al., 1984; Taylor and Whitelaw, 2001; Trobacher,

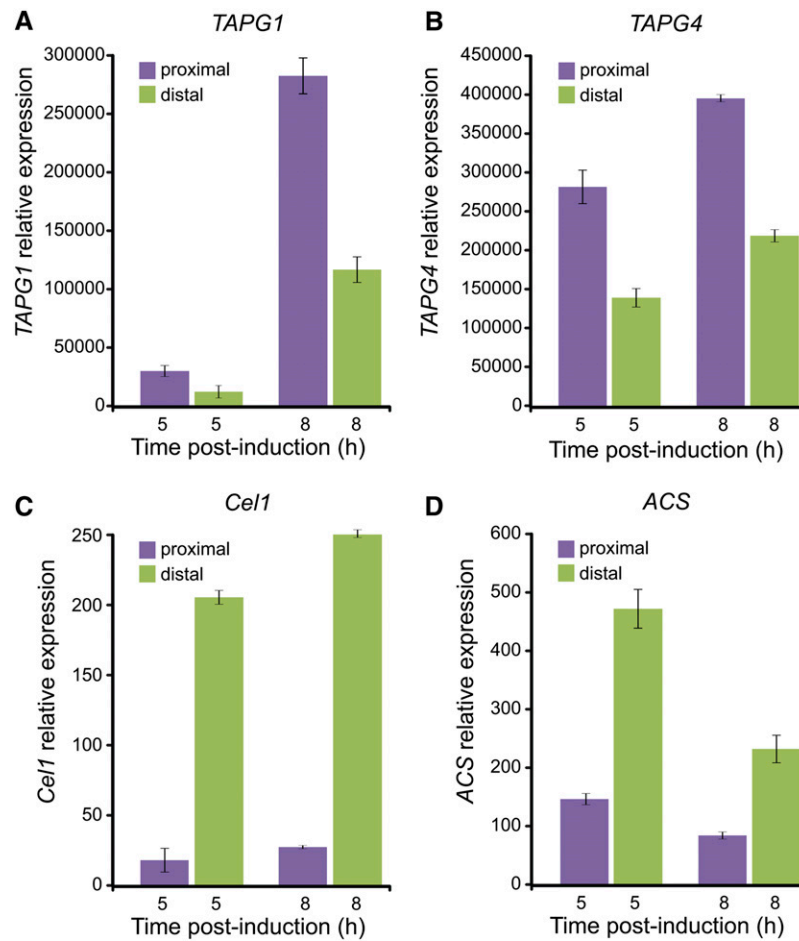


Figure 9. *TAPG1*, *TAPG4*, *Cel1*, and *ACS* Genes Are Differentially Expressed during Pedicel Abscission in Tissues Localized Distal or Proximal to the Tomato Flower AZ.

Tissues were sampled at the indicated time points following flower removal for abscission induction from either the proximal or distal side of the flower AZ, and extracted RNA was used for quantitative real-time PCR. Error bars correspond to \pm SD. The accession IDs for the examined genes are as follows: *Cel1*, U13054; *TAPG1*, AF001000; *TAPG4*, U70481; and *ACS*, M34289.

[See online article for color version of this figure.]

2009). Ethylene regulates the late stage 3 of abscission; however, the specific tissue in which it is produced is not known. It is possible that biosynthesis of abscission-related ethylene occurs in the cells located in the distal side of the AZ. Our observation that the *ACS* transcript, associated with ethylene biosynthesis, is accumulated to a higher level in the distal side of the AZ compared with the proximal side (Figure 9D), is in accordance with this possibility. Coupling between the elevated ethylene biosynthesis in those AZ distal cells and the PCD process may exist. In such a case, inhibition of PCD would result in a lower level of ethylene biosynthesis and a delay in the progress of abscission. Experiments are underway to examine this hypothesis.

Abscission Is Impeded in Transgenic Plants Overexpressing Antiapoptotic Proteins

Members of the IAP family function as cell death suppressors in eukaryotes (Deveraux and Reed, 1999; Yang and Li, 2000). IAPs

share a conserved domain (BIR), which binds caspases in mammals and is required for antiapoptotic activity. The possibility of limiting the advancement of plant PCD processes by heterologous overexpression of antiapoptotic genes has been reported (Dickman et al., 2001). Expression of the fall armyworm IAP-encoding gene has been shown to inhibit apoptosis in human cells and to be a specific inhibitor of mammalian caspase-9 (Huang et al., 2000). Overexpression in plants of the antiapoptotic proteins Sf IAP or P35 has been found to inhibit PCD, which is otherwise induced in response to abiotic stresses and to confer elevated tolerance toward these stresses (Lincoln et al., 2002; del Pozo and Lam, 2003; Danon et al., 2004; Wang et al., 2009; Wijayanto et al., 2009; Kabbage et al., 2010; Li et al., 2010). We observed a significant delay of both leaf and flower abscission in plants overexpressing these very different antiapoptotic proteins, Sf IAP and P35 (Figure 8). These results support the hypothesis that the normal progress of the observed PCD in the AZ is functionally involved in the abscission process.

Differences between the Tissues Localized Proximal and Distal to the AZ

PCD as well as the expression of *LX*, *TBN1*, *Cel1*, and *ACS* genes are induced on the distal side of the AZ (Figures 3E, 3F, 4, 6C, 9C, and 9D), indicating an asymmetry between the cells on the two opposite sides, which may be involved in the late execution stage of abscission. The induction of cell wall hydrolase activity has long been known to be a dominant feature of this execution stage. Previous observations are consistent with the differential expression patterns of abscission-related cell wall hydrolase genes in tissues located on the two sides of the AZ (Tucker et al., 1984; Lashbrook et al., 1994; del Campillo and Bennett, 1996; Hong et al., 2000; Wang et al., 2005). However, unlike the above-mentioned genes, the cell wall PG genes *TAPG1* and *TAPG4* were asymmetrically expressed during flower abscission, with stronger expression on the proximal side of the AZ (Figures 9A and 9B).

PGs are thought to be responsible for the degradation of pectin in the cell wall and middle lamella of plant cells and are encoded by a multimeric gene family (Kalaitzis et al., 1997; González-Carranza et al., 2002, 2007; Kim et al., 2006). Inhibition of the *PG* gene expression results in inhibition of abscission and dehiscence (Jiang et al., 2008; Ogawa et al., 2009). Cellulases are also thought to be involved in cell wall degradation during abscission, and inhibition of the tomato cellulase gene expression results in partial inhibition of abscission (Lashbrook et al., 1998; Brummell et al., 1999). However, when the tomato *Cel1* was silenced, alone or in combination with *Cel2*, no effect on abscission was observed (Jiang et al., 2008). The significance of the observed opposite differential expression of the *TAPGs* and *Cel1* between the distal and proximal sides of the flower AZ (Figures 9A to 9C) is not yet understood. It is possible that the *Cel1* gene is specifically involved in the observed PCD process on the distal side of the AZ, while other members of the cellulase family are involved in cell wall metabolism during cell separation in the AZ. Expression of cellulase genes has been associated with PCD processes (Kawase, 1979; del Campillo et al., 2004; Evans, 2004; Shani et al., 2006; Gunawardena et al., 2007).

The underlying details specifying the differences between proximal and distal AZ tissues with respect to abscission-related processes are not yet clear. It is clear that differences do exist and that the occurrence of PCD on the distal side is likely to be relevant. The asymmetry observed between the tissues on either side of the AZ is also supported by the observed cellular structure and morphology of the proximal tissue, which shows extensive membrane trafficking associated with an elaborate plasmodesmal system (Figure 6). Similar observations were reported in early studies on abscission of tobacco and tomato flowers (Jensen and Valdovinos, 1967, 1968). However, the membrane invaginations in the leaf AZ of *Phaseolus vulgaris* (Webster, 1973) have gained renewed attention of late, with regard to their association with multivesicular bodies (MVBs) and PBs. MVBs are redirected to the plasma membrane, where they release their contents, including internal vesicles captured in PBs, into the extracellular space by membrane fusion (reviewed in An et al., 2007). Similar structures have been recently described during *Arabidopsis* floral organ abscission (Liljegren et al., 2009). The authors

proposed that the protein NEVERSHED, which colocalizes with these compartments, is required for cell separation. In addition, MVBs and PBs have been shown during embryogenesis (Goh et al., 2007) as well as in virus-induced local lesions (McMullen et al., 1977) and barley (*Hordeum vulgare*) leaf cells upon fungal infection (An et al., 2006, 2007). It has been suggested that MVBs and PBs participate in the secretion of building blocks for cell wall appositions (An et al., 2006). Here, we showed the occurrence of PBs in cells on the proximal side of the AZ fracture (Figures 5E and 5F), which might play a similar role during the development of a protective layer at the surface of the exposed tissue, following the release of cells at the site of leaf detachment from the plant body. MVBs might deliver endocytosed cell wall material to the cell surface, where its rapid deposition then occurs through the PBs.

In conclusion, our data show that both PCD and *LX* expression are clearly associated with the abscission process, both in leaves and flowers, primarily during the terminal stages when cell separation is executed. *LX* expression is required for the normal progression of organ abscission. Our observations showing that when plants overexpress cytoprotective antiapoptosis genes, abscission is impeded support involvement of PCD in abscission. Since *LX* is associated with PCD, it is reasonable to hypothesize that normal levels of *LX* are required for PCD to occur, which in turn is required for the normal progress of abscission.

METHODS

Plant Growth Conditions and Treatments

Tomato (*Solanum lycopersicum* cv VF36) was used throughout this study unless otherwise specified. Tomato seeds were germinated on perlite support at 28°C in the dark, and after 3 d, seedlings were transferred to the light. When cotyledons were fully developed, the seedlings were transferred to 300-mL containers filled with HR1 artificial soil (Hagarin Ltd.). The plants were grown in either a greenhouse under a controlled temperature of 25°C and natural daylight or in growth chambers at 25°C and a 16/8-h day/night cycle. For auxin treatment, detached leaves were immersed in water containing 200 μM of the synthetic auxin 2,4-D and 0.1% (v/v) Tween 80 for 30 min. Ethylene application was performed by incubating the detached leaves in sealed transparent Perspex containers fitted with inlet and outlet ports and connected to a flow-through system. Air (control) or 5 μL/L ethylene in air was bubbled through sterile water to maintain humidity and then continuously flowed through the jars at a rate of 100 mL/min. For the combined hormone treatment, ethylene flow was applied 24 h after the auxin pretreatment to allow auxin action before ethylene application.

Abscission was induced by removing either the flower or the leaf blade as previously described (Roberts et al., 1984; Lers et al., 2006; Meir et al., 2006, 2010). Leaf abscission experiments were performed in planta. For induction, the leaf blades of up to four bottom leaves were removed with a sharp razor, leaving most of the petioles intact. For abscission acceleration, ethylene was applied 36 h later to the debladed tomato plants by placing them for 24 h in sealed containers as described above. In experiments designed to follow flower abscission, flowers at similar levels of development were used. A day before the experiment, all opened flowers were removed from the plants, and only flowers that opened the night before the initiation of the experiments were used. Young flowers that had not reached full opening were also excluded. Induced-abscission

experiments in flowers were performed either in planta or in vitro using detached clusters of flowers kept in water throughout the experiments (Meir et al., 2010). In both systems, flowers were cut at their base with a sharp razor to induce pedicle abscission. When full separation of the abscising organ did not occur, completion of pedicel or petiole abscission was performed by carefully touching the edge of the examined tissue.

SDS-PAGE, Immunoblot Analyses, and Enzyme Activity Gel Assays

Proteins for immunoblot analysis were extracted from nine 7-mm-diameter leaf discs or from 30 pooled stem segments (1 to 2 mm long, total of ~30 mg). The tissue was homogenized in the presence of 150 μ L extraction buffer (50 mM Tris-HCl, pH 7.5, 0.1% [w/v] SDS, 10% [w/v] polyvinylpyrrolidone, and 1 mM phenylmethylsulfonyl fluoride) in a micro-tube by means of a fitted pestle and a motorized drill. Following 15 min of centrifugation at 4°C, the soluble protein extract was assayed for protein content by Bradford assay (Bio-Rad) and stored at -80°C. Protein extracts of 5 to 10 μ g were mixed with sample buffer and boiled for 5 min before separation on a 15% SDS-polyacrylamide gel (Laemmli, 1970). Separated proteins were blotted onto nitrocellulose membranes with a gel blotter (Bio-Rad). Membranes were blocked with a solution containing 5% (v/v) nonfat milk and 0.1% Tween 20 in Tris-buffered saline for 60 min. The anti-LX serum (Lers et al., 2006) was diluted 1:2000 in the blocking solution and incubated with the membrane for 12 to 16 h at 4°C. The membrane was washed for 30 min in several changes of Tris-buffered saline containing 0.1% Tween 20. The secondary antibody was goat anti-rabbit IgG:horseradish peroxidase conjugate (Bio-Rad), which was diluted 1:50,000 in blocking solution and incubated with the membrane for 1 h at room temperature. For signal detection, the EZ-ECL chemiluminescent kit (Biological Industries) was used. Activity gel assays for the identification of nuclease and protease activity following SDS-PAGE were performed as described previously (Jiang et al., 1999; Lers et al., 2001). Proteins were extracted from the AZ-containing tissue or separately from the distal and proximal tissues relative to the AZ fracture at a late stage of abscission and subjected to the activity gel assay. As a control, proteins were extracted from nearby pedicel tissue.

Quantitative Real-Time PCR and Microarray Analyses

Flower samples for AZ and NAZ tissues were collected as described above. Total RNA was isolated using the Spectrum plant total RNA kit (Sigma-Aldrich) and treated with TURBO DNase (Ambion) according to the manufacturer's instructions. RNA was reverse transcribed with the ReverAid first-strand cDNA synthesis kit (Fermentas) using oligo(dT) primers. The quantitative real-time PCR was performed with a Corbett Rotor-Gene 3000 (Corbett Life Research) using Absolute blue QPCR SYBR green mix (Thermo Scientific) and gene-specific primers. The primers were designed using PrimerQuest software (<http://eu.idtdna.com/Scitools/Applications/Primerquest/>) and are listed in Supplemental Table 2 online. Expression values were normalized to the individual expression of the *actin* gene. To analyze *LX* ribonuclease during leaf abscission, the AZs were separated into proximal and distal parts, and thin layers of tissue were excised from each using a scalpel and frozen in liquid nitrogen. Samples were homogenized in TissueLyser (Qiagen). RNA was extracted using the RNeasy Micro kit (Qiagen), and cDNA was synthesized using the High Capacity cDNA archive kit (Applied Biosystems). The quantitative real-time PCR was performed in an ABI PRISM 7900 HT Fast Real-Time PCR (Applied Biosystems) with the primers listed in Supplemental Table 1 online using SYBR green (Applied Biosystems). *LX* expression was normalized relative to its expression in intact controls and the expression of a reference gene, *COX* (for cytochrome oxidase). The expression data were analyzed by the relative standard curve method using the $\Delta\Delta$ cycle threshold method (Livak and Schmittgen, 2001). All

experiments were carried with nontemplate control and repeated for three biological experiments. Microarray analysis of gene expression in flower AZ and the effect of 1-MCP and IAA treatments were extracted from the AZ microarray analysis performed as described by Meir et al. (2010).

Transmission Electron Microscopy

At 0, 4, 24, and 48 h after the 24-h ethylene treatment, treated and untreated control plants were sampled. Samples of untreated plants were taken at different times of the day to minimize the influence of the circadian rhythm. Blocks of tissue with the longest side measuring ~2 mm, containing the AZ, were fixed in 3% (w/v) glutaraldehyde (in 0.08 M phosphate buffer, pH 7.2) and postfixed for 12 h in 1% (w/v) osmium tetroxide in the same buffer. Embedded samples (agar 100 resin) were cut into ultrathin sections (70 to 90 nm) and stained in a 3% (w/v) water solution of uranyl acetate and water solution of lead citrate. Samples were observed with a CM 100 transmission electron microscope (Philips) operating at 80 kV, and images were recorded with a Bioscan CCD camera using Digital Micrograph software (Gatan).

Tissue Staining with EB, DAPI, and DCF

AZ and adjacent tissues were isolated from control or abscission-induced tomato leaves or flowers. After the indicated induction time, longitudinal sections were cut with a sharp razor blade to obtain a lateral view of the AZ. In addition, top-view images of the AZ plane were obtained to observe the fracture plane tissue located proximal and distal to the AZ cell layers, by applying gentle force to separate the AZ. The different dyes were applied on fresh tissue. Fluorescent dyes were diluted in phosphate buffer (50 mM) and visualized using an Olympus IX81 inverted confocal laser scanning microscope (Fluoview 500) or an MZ FLIII binocular microscope (Leica Microsystems). Pictures were taken using a Leica DC200 digital imaging system. Nuclei were stained using DAPI (Sigma-Aldrich) and observed following UV excitation. Staining for ROS was performed using DCF (Sigma-Aldrich) with excitation at 488 nm and emission at 515 to 540 nm.

Cell viability was evaluated by EB staining (Baker and Mock, 1994). Tissues were stained in a 0.1% (v/v) aqueous solution of EB for 3 min and washed for at least 30 min, with frequent water changes.

Histological Tissue Section Preparation for TUNEL Assay and LX Immunolocalization

Leaf AZs were sampled by excising segments of stem with leaf petioles at different times from the start of abscission induction. Samples were fixed in FAA (3.7% formaldehyde, 50% ethanol, and 5% glacial acetic acid, [v/v]) overnight at 4°C, dehydrated in a series of ethanol and tertiary butyl alcohol, embedded in Paraplast Plus (Sherwood Medical), and sectioned longitudinally on a rotary microtome (Autocut 2040; Reichert-Jung).

Detection of Nuclear DNA Fragmentation by TUNEL Assay

TUNEL assay was performed on Paraplast Plus-embedded tissue sections using an ApopTag Fluorescein *In Situ* Apoptosis Detection Kit (Chemicon International), essentially following the manufacturer's protocol. Briefly, rehydrated sections were treated with 125 μ g/mL pronase E (Sigma-Aldrich) for 30 min at room temperature, incubated in a mixture of digoxigenin-labeled deoxynucleotides and terminal deoxynucleotidyl transferase for 60 min at 37°C, followed by incubation with fluorescein-labeled antidigoxigenin antibodies. Slides were washed with phosphate-buffered saline and mounted in FluoroMount (Sigma-Aldrich) with 600 nM DAPI. The fluorescein-labeled nuclei were observed with blue-light excitation (excitation 450- to 490-nm band-pass; emission 515-nm

long-pass), and DAPI fluorescence of all nuclei was observed with UV excitation (excitation 365/12-nm band-pass; emission 397-nm long-pass) and photographed with the AxioCam HRc color digital camera (Carl Zeiss Vision).

LX Immunolocalization

Paraplast Plus-embedded tissue sections were placed on Superfrost Ultra Plus slides (Menzel-Gläser). Sections were dewaxed in xylene and rehydrated in an ethanol series to distilled water. Antigen retrieval was performed by incubating slides in sodium citrate buffer (10 mM sodium citrate, pH 6.0) for 15 min in a boiling water bath and washed gently in running tap water. Sections were incubated in blocking solution (1× TRIS buffered saline, pH 7.6, 1% [w/v] BSA, 0.025% [v/v] Triton X-100, and 5% [v/v] normal goat serum) for 1 h at room temperature. Blocking solution was then replaced with anti-LX serum (Lers et al., 2006) diluted 1:10⁵ in blocking solution and incubated overnight at 4°C. Preimmune serum was used instead of anti-LX serum for negative controls. Sections were washed the next day in 1× TRIS buffered saline for 5 min, followed by three washes in distilled water with 0.2% Tween 20. Sections were then incubated with alkaline phosphatase-labeled anti-rabbit antibodies (Jackson ImmunoResearch), diluted 1:1000 in blocking solution, for 1 h at room temperature, followed by washing as above. Staining was developed in nitro blue tetrazolium chloride/5-bromo-4-chloro-3-indolyl-phosphate substrate solution (Roche Diagnostics) following the manufacturer's instructions, washed with water, dehydrated quickly through an ethanol series and xylene, and mounted in Permount (Electron Microscopy Sciences). The purple precipitate at the sites of primary antibody binding to LX protein was photographed using a Zeiss AxioImager Z1 microscope and AxioCam HRc color digital camera.

Accession Numbers

Sequence data from this article can be found in the GenBank/EMBL data libraries under the following accession numbers: *LX*, X79338; *SBT3*, AJ006376; *Cys protease*, BT014429; *Cel1*, U13054; *NADPH oxidase*, AF088276; *pirin*, AF15400; *Sphingosine-1-phosphate lyase*, AW030786; *TAPG1*, AF001000; *TAPG4*, U70481, AF001002; *TBN1*, AM238701; *ACS*, M34289; and *Actin*, AB199316.

Supplemental Data

The following materials are available in the online version of this article.

Supplemental Figure 1. Effects of Auxin and/or Ethylene on Induction of LX Protein in Tomato Leaves.

Supplemental Figure 2. Effect of External Ethylene on Induction of LX Protein in Wild-Type Tomato Flower AZ.

Supplemental Figure 3. Effect of External Ethylene on Abscission of Flower Pedicels in Wild-Type and *LX*-Inhibited Transgenic Tomato Plants.

Supplemental Figure 4. Evans Blue Staining Indicates Cell Death in the Abscission Zone of Tomato and Tree Tobacco Leaves and *Arabidopsis* Flower Organs.

Supplemental Figure 5. TUNEL and DAPI Staining of Tomato Leaf Abscission Zone Area Not Induced for Abscission.

Supplemental Figure 6. Transmission Electron Micrographs of Cells in Tomato Leaf Abscission Zone Showing Ultrastructural Changes from 4 to 48 h after Induction of Abscission by Leaf Deblading and Ethylene Treatment.

Supplemental Figure 7. Induction of Expression of PCD-Associated Genes in the Tomato Flower Abscission Zone following Induction of Abscission by Flower Removal.

Supplemental Table 1. Time Course of Ultrastructural Changes in the Cells of the Leaf Abscission Zone after Abscission Induction by Leaf Deblading and Ethylene Treatment.

Supplemental Table 2. Primers Used for Quantitative Real-Time PCR Analyses.

ACKNOWLEDGMENTS

We thank James E. Lincoln (University of California, Davis) for the *p35*-transgenic line. This research was supported by Research Grant 1019/06 from the Israel Science Foundation of the Israel Academy of Sciences; Research Grants IS-3645-04 and IS-4073-07C from BARD, the U.S.–Israel Binational Agricultural Research and Development Fund; and Research Grant J4-9738 from the Slovenian Research Agency. This article is contribution number 611/11 from the Agricultural Research Organization, The Volcani Center, Israel.

AUTHOR CONTRIBUTIONS

T.B.-D., M.D., and A.L. designed the research. T.B.-D., A.K., M.T.Z., M.P.N., S.M., S.B., L.S., and A.L. performed the research. T.B.-D., M.D., S.M., S.P.-H., N.O., M.B.D., and A.L. analyzed data. M.D., S.M., S.P.-H., N.O., M.B.D., and A.L. wrote the article.

Received October 11, 2011; revised October 11, 2011; accepted November 17, 2011; published November 29, 2011.

REFERENCES

- Abeles, F.B., and Rubinstein, B.** (1964). Regulation of ethylene evolution and leaf abscission by auxin. *Plant Physiol.* **39**: 963–969.
- Agustí, J., Merelo, P., Cercós, M., Tadeo, F.R., and Talón, M.** (2009). Comparative transcriptional survey between laser-microdissected cells from laminar abscission zone and petiolar cortical tissue during ethylene-promoted abscission in citrus leaves. *BMC Plant Biol.* **9**: 127.
- Aleksandrushkina, N.I., and Vanyushin, B.F.** (2009). Endonucleases and their involvement in plant apoptosis. *Russ. J. Plant Physiol.* **56**: 291–305.
- An, Q., Ehlers, K., Kogel, K.H., van Bel, A.J.E., and Hüchelhoven, R.** (2006). Multivesicular compartments proliferate in susceptible and resistant MLA12-barley leaves in response to infection by the biotrophic powdery mildew fungus. *New Phytol.* **172**: 563–576.
- An, Q., van Bel, A.J., and Hüchelhoven, R.** (2007). Do plant cells secrete exosomes derived from multivesicular bodies? *Plant Signal. Behav.* **2**: 4–7.
- Baker, C.J., and Mock, N.M.** (1994). An improved method for monitoring cell-death in cell-suspension and leaf disc assays using Evans Blue. *Plant Cell Tissue Organ Cult.* **39**: 7–12.
- Belfield, E.J., Ruperti, B., Roberts, J.A., and McQueen-Mason, S.** (2005). Changes in expansin activity and gene expression during ethylene-promoted leaflet abscission in *Sambucus nigra*. *J. Exp. Bot.* **56**: 817–823.
- Binder, B.M., and Patterson, S.E.** (2009). Ethylene-dependent and independent regulation of abscission. *Stewart Postharvest Rev.* **5**: 1–10.
- Bonneau, L., Ge, Y., Drury, G.E., and Gallois, P.** (2008). What happened to plant caspases? *J. Exp. Bot.* **59**: 491–499.
- Bozhkov, P., and Jansson, C.** (2007). Autophagy and cell-death proteases in plants: Two wheels of a funeral cart. *Autophagy* **3**: 136–138.
- Brummell, D.A., Hall, B.D., and Bennett, A.B.** (1999). Antisense

- suppression of tomato endo-1,4-beta-glucanase *Cel2* mRNA accumulation increases the force required to break fruit abscission zones but does not affect fruit softening. *Plant Mol. Biol.* **40**: 615–622.
- Burch-Smith, T.M., Stonebloom, S., Xu, M., and Zambryski, P.C.** (2011). Plasmodesmata during development: Re-examination of the importance of primary, secondary, and branched plasmodesmata structure versus function. *Protoplasma* **248**: 61–74.
- Cacas, J.L.** (2010). Devil inside: Does plant programmed cell death involve the endomembrane system? *Plant Cell Environ.* **33**: 1453–1473.
- Cai, S.Q., and Lashbrook, C.C.** (2008). Stamen abscission zone transcriptome profiling reveals new candidates for abscission control: enhanced retention of floral organs in transgenic plants overexpressing *Arabidopsis* ZINC FINGER PROTEIN2. *Plant Physiol.* **146**: 1305–1321.
- Castillo-Olamendi, L., Bravo-Garcia, A., Moran, J., Rocha-Sosa, M., and Porta, H.** (2007). AtMCP1b, a chloroplast-localised metacaspase, is induced in vascular tissue after wounding or pathogen infection. *Funct. Plant Biol.* **34**: 1061–1071.
- Cho, H.T., and Cosgrove, D.J.** (2000). Altered expression of expansin modulates leaf growth and pedicel abscission in *Arabidopsis thaliana*. *Proc. Natl. Acad. Sci. USA* **97**: 9783–9788.
- Cho, S.K., Larue, C.T., Chevalier, D., Wang, H.C., Jinn, T.L., Zhang, S.Q., and Walker, J.C.** (2008). Regulation of floral organ abscission in *Arabidopsis thaliana*. *Proc. Natl. Acad. Sci. USA* **105**: 15629–15634.
- Coupe, S.A., Taylor, J.E., and Roberts, J.A.** (1995). Characterisation of an mRNA encoding a metallothionein-like protein that accumulates during ethylene-promoted abscission of *Sambucus nigra* L. leaflets. *Planta* **197**: 442–447.
- Coupe, S.A., Taylor, J.E., and Roberts, J.A.** (1997). Temporal and spatial expression of mRNAs encoding pathogenesis-related proteins during ethylene-promoted leaflet abscission in *Sambucus nigra*. *Plant Cell Environ.* **20**: 1517–1524.
- Danon, A., Rotari, V.I., Gordon, A., Mailhac, N., and Gallois, P.** (2004). Ultraviolet-C overexposure induces programmed cell death in *Arabidopsis*, which is mediated by caspase-like activities and which can be suppressed by caspase inhibitors, p35 and Defender against Apoptotic Death. *J. Biol. Chem.* **279**: 779–787.
- del Campillo, E., Abdel-Aziz, A., Crawford, D., and Patterson, S.E.** (2004). Root cap specific expression of an endo-beta-1,4-D-glucanase (cellulase): A new marker to study root development in *Arabidopsis*. *Plant Mol. Biol.* **56**: 309–323.
- del Campillo, E., and Bennett, A.B.** (1996). Pedicel breakstrength and cellulase gene expression during tomato flower abscission. *Plant Physiol.* **111**: 813–820.
- del Pozo, O., and Lam, E.** (2003). Expression of the baculovirus p35 protein in tobacco affects cell death progression and compromises N gene-mediated disease resistance response to Tobacco mosaic virus. *Mol. Plant Microbe Interact.* **16**: 485–494.
- Despa, F.** (2009). Dilation of the endoplasmic reticulum in beta cells due to molecular overcrowding? Kinetic simulations of extension limits and consequences on proinsulin synthesis. *Biophys. Chem.* **140**: 115–121.
- Deveraux, Q.L., and Reed, J.C.** (1999). IAP family proteins—Suppressors of apoptosis. *Genes Dev.* **13**: 239–252.
- Dickman, M.B., Park, Y.K., Oltersdorf, T., Li, W., Clemente, T., and French, R.** (2001). Abrogation of disease development in plants expressing animal antiapoptotic genes. *Proc. Natl. Acad. Sci. USA* **98**: 6957–6962.
- Evans, D.E.** (2004). Aerenchyma formation. *New Phytol.* **161**: 35–49.
- Evensen, K.B., Page, A.M., and Stead, A.D.** (1993). Anatomy of ethylene-induced petal abscission in *Pelargonium x Hortorum*. *Ann. Bot. (Lond.)* **71**: 559–566.
- Eyal, Y., Meller, Y., Lev-Yadun, S., and Fluhr, R.** (1993). A basic-type PR-1 promoter directs ethylene responsiveness, vascular and abscission zone-specific expression. *Plant J.* **4**: 225–234.
- Farage-Barhom, S., Burd, S., Sonogo, L., Perl-Treves, R., and Lers, A.** (2008). Expression analysis of the *BFN1* nuclease gene promoter during senescence, abscission, and programmed cell death-related processes. *J. Exp. Bot.* **59**: 3247–3258.
- Gadjev, I., Stone, J.M., and Gechev, T.S.** (2008). Programmed cell death in plants: New insights into redox regulation and the role of hydrogen peroxide. In *International Review of Cell and Molecular Biology*, Vol. 270, K.W. Jeon, ed (San Diego, CA: Elsevier Academic Press), pp. 87–144.
- Gavrieli, Y., Sherman, Y., and Ben-Sasson, S.A.** (1992). Identification of programmed cell death *in situ* via specific labeling of nuclear DNA fragmentation. *J. Cell Biol.* **119**: 493–501.
- Goh, T., Uchida, W., Arakawa, S., Ito, E., Dainobu, T., Ebine, K., Takeuchi, M., Sato, K., Ueda, T., and Nakano, A.** (2007). VPS9a, the common activator for two distinct types of Rab5 GTPases, is essential for the development of *Arabidopsis thaliana*. *Plant Cell* **19**: 3504–3515.
- Ghosh, S., Mahoney, S.R., Penterman, J.N., Peirson, D., and Dumbroff, E.B.** (2001). Ultrastructural and biochemical changes in chloroplasts during *Brassica napus* senescence. *Plant Physiol. Biochem.* **39**: 777–784.
- González-Carranza, Z.H., Elliott, K.A., and Roberts, J.A.** (2007). Expression of polygalacturonases and evidence to support their role during cell separation processes in *Arabidopsis thaliana*. *J. Exp. Bot.* **58**: 3719–3730.
- González-Carranza, Z.H., Whitelaw, C.A., Swarup, R., and Roberts, J.A.** (2002). Temporal and spatial expression of a polygalacturonase during leaf and flower abscission in oilseed rape and *Arabidopsis*. *Plant Physiol.* **128**: 534–543.
- Greenberg, J., Goren, R., and Rivov, J.** (1975). Role of cellulase and polygalacturonase in abscission of young and mature Shamouti orange fruits. *Physiol. Plant.* **34**: 1–7.
- Guamet, J.J., Pichersky, E., and Nooden, L.D.** (1999). Mass exodus from senescing soybean chloroplasts. *Plant Cell Physiol.* **40**: 986–992.
- Gunawardena, A.H.L.A.N., Greenwood, J.S., and Dengler, N.G.** (2007). Cell wall degradation and modification during programmed cell death in lace plant, *Aponogeton madagascariensis* (Aponogetonaceae). *Am. J. Bot.* **94**: 1116–1128.
- Helm, M., Schmid, M., Hierl, G., Terneus, K., Tan, L., Lottspeich, F., Kieliszewski, M.J., and Gietl, C.** (2008). KDEL-tailed cysteine endopeptidases involved in programmed cell death, intercalation of new cells, and dismantling of extensin scaffolds. *Am. J. Bot.* **95**: 1049–1062.
- Henry, E.W., Valdovinos, J.G., and Jensen, T.E.** (1974). Peroxidases in tobacco abscission zone tissue. 2. Time course studies of peroxidase activity during ethylene-induced abscission. *Plant Physiol.* **54**: 192–196.
- Hoefert, L.L.** (1975). Tubules in dilated cisternae of endoplasmic reticulum of *Thlaspi arvense* (Cruciferae). *Am. J. Bot.* **62**: 756–760.
- Hong, S.B., Sexton, R., and Tucker, M.L.** (2000). Analysis of gene promoters for two tomato polygalacturonases expressed in abscission zones and the stigma. *Plant Physiol.* **123**: 869–881.
- Huang, Q., Deveraux, Q.L., Maeda, S., Salvesen, G.S., Stennicke, H.R., Hammock, B.D., and Reed, J.C.** (2000). Evolutionary conservation of apoptosis mechanisms: Lepidopteran and baculoviral inhibitor of apoptosis proteins are inhibitors of mammalian caspase-9. *Proc. Natl. Acad. Sci. USA* **97**: 1427–1432.
- Ito, J., and Fukuda, H.** (2002). ZEN1 is a key enzyme in the degradation of nuclear DNA during programmed cell death of tracheary elements. *Plant Cell* **14**: 3201–3211.
- Jarvis, M.C., Briggs, S.P.H., and Knox, J.P.** (2003). Intercellular adhesion and cell separation in plants. *Plant Cell Environ.* **26**: 977–989.
- Jensen, T.E., and Valdovinos, J.G.** (1967). Fine structure of abscission zones. I. Abscission zones of the pedicels of tobacco and tomato flowers at anthesis. *Planta* **77**: 298–318.
- Jensen, T.E., and Valdovinos, J.G.** (1968). Fine structure of abscission

- zones III. Cytoplasmic changes in abscising pedicels of tobacco and tomato flowers. *Planta* **83**: 303–313.
- Jiang, C.Z., Lu, F., Imsabai, W., Meir, S., and Reid, M.S.** (2008). Silencing polygalacturonase expression inhibits tomato petiole abscission. *J. Exp. Bot.* **59**: 973–979.
- Jiang, W.B., Lers, A., Lomaniec, E., and Aharoni, N.** (1999). Senescence-related serine protease in parsley. *Phytochemistry* **50**: 377–382.
- Kabbage, M., Li, W., Chen, S.R., and Dickman, M.B.** (2010). The E3 ubiquitin ligase activity of an insect anti-apoptotic gene (*SflAP*) is required for plant stress tolerance. *Physiol. Mol. Plant Pathol.* **74**: 351–362.
- Kalaitzis, P., Solomos, T., and Tucker, M.L.** (1997). Three different polygalacturonases are expressed in tomato leaf and flower abscission, each with a different temporal expression pattern. *Plant Physiol.* **113**: 1303–1308.
- Kawase, M.** (1979). Role of cellulase in aerenchyma development in sunflower. *Am. J. Bot.* **66**: 183–190.
- Kim, J., Shiu, S.H., Thoma, S., Li, W.H., and Patterson, S.E.** (2006). Patterns of expansion and expression divergence in the plant polygalacturonase gene family. *Genome Biol.* **7**: R87.
- Kitajima, A., Sasagawa, K., and Hasegawa, K.** (2003). Development of the abscission zone and morphological changes of abscission cells in the abscission process of persimmon fruit. *Acta Hort.* **601**: 85–87.
- Köck, M., Stenzel, I., and Zimmer, A.** (2006). Tissue-specific expression of tomato Ribonuclease *LX* during phosphate starvation-induced root growth. *J. Exp. Bot.* **57**: 3717–3726.
- Laemmli, U.K.** (1970). Cleavage of structural proteins during the assembly of the head of bacteriophage T4. *Nature* **227**: 680–685.
- Lam, E.** (2008). Programmed cell death in plants: Orchestrating an intrinsic suicide program within walls. *Crit. Rev. Plant Sci.* **27**: 413–423.
- Lashbrook, C.C., Giovannoni, J.J., Hall, B.D., Fischer, R.L., and Bennett, A.B.** (1998). Transgenic analysis of tomato endo-beta-1,4-glucanase gene function. Role of *Cel1* in floral abscission. *Plant J.* **13**: 303–310.
- Lashbrook, C.C., Gonzalez-Bosch, C., and Bennett, A.B.** (1994). Two divergent endo-beta-1,4-glucanase genes exhibit overlapping expression in ripening fruit and abscising flowers. *Plant Cell* **6**: 1485–1493.
- Lehmann, K., Hause, B., Altmann, D., and Köck, M.** (2001). Tomato ribonuclease *LX* with the functional endoplasmic reticulum retention motif HDEF is expressed during programmed cell death processes, including xylem differentiation, germination, and senescence. *Plant Physiol.* **127**: 436–449.
- Lers, A., Khalchitski, A., Lomaniec, E., Burd, S., and Green, P.J.** (1998). Senescence-induced RNases in tomato. *Plant Mol. Biol.* **36**: 439–449.
- Lers, A., Lomaniec, E., Burd, S., and Khalchitski, A.** (2001). The characterization of LeNUC1, a nuclease associated with leaf senescence of tomato. *Physiol. Plant.* **112**: 176–182.
- Lers, A., Sonogo, L., Green, P.J., and Burd, S.** (2006). Suppression of *LX* ribonuclease in tomato results in a delay of leaf senescence and abscission. *Plant Physiol.* **142**: 710–721.
- Leslie, M.E., Lewis, M.W., and Liljegren, S.J.** (2007). Organ abscission. In *Plant Cell Separation and Adhesion*, J.A. Roberts, and Z.H. González-Carranza, eds (Oxford, UK: Blackwell Publishing), pp. 106–136.
- Lewis, M.W., Leslie, M.E., and Liljegren, S.J.** (2006). Plant separation: 50 ways to leave your mother. *Curr. Opin. Plant Biol.* **9**: 59–65.
- Li, W., Kabbage, M., and Dickman, M.B.** (2010). Transgenic expression of an insect inhibitor of apoptosis gene, *SflAP*, confers abiotic and biotic stress tolerance and delays tomato fruit ripening. *Physiol. Mol. Plant Pathol.* **74**: 363–375.
- Liljegren, S.J., Leslie, M.E., Darnielle, L., Lewis, M.W., Taylor, S.M., Luo, R.B., Geldner, N., Chory, J., Randazzo, P.A., Yanofsky, M.F., and Ecker, J.R.** (2009). Regulation of membrane trafficking and organ separation by the NEVERSHED ARF-GAP protein. *Development* **136**: 1909–1918.
- Lincoln, J.E., Richael, C., Overduin, B., Smith, K., Bostock, R., and Gilchrist, D.G.** (2002). Expression of the antiapoptotic baculovirus p35 gene in tomato blocks programmed cell death and provides broad-spectrum resistance to disease. *Proc. Natl. Acad. Sci. USA* **99**: 15217–15221.
- Livak, K.J., and Schmittgen, T.D.** (2001). Analysis of relative gene expression data using real-time quantitative PCR and the 2⁻(Delta Delta C(T)) Method. *Methods* **25**: 402–408.
- Macnish, A.J., Irving, D.E., Joyce, D.C., Vithanage, V., and Wearing, A.H.** (2005). Anatomy of ethylene-induced floral-organ abscission in *Chamelaucium uncinatum* (Myrtaceae). *Aust. J. Bot.* **53**: 119–131.
- Marutani, T., Yamamoto, A., Nagai, N., Kubota, H., and Nagata, K.** (2004). Accumulation of type IV collagen in dilated ER leads to apoptosis in Hsp47-knockout mouse embryos via induction of CHOP. *J. Cell Sci.* **117**: 5913–5922.
- Matousek, J., Kozlová, P., Orctová, L., Schmitz, A., Pesina, K., Bannach, O., Diermann, N., Steger, G., and Riesner, D.** (2007). Accumulation of viroid-specific small RNAs and increase in nucleolytic activities linked to viroid-caused pathogenesis. *Biol. Chem.* **388**: 1–13.
- McKim, S.M., Stenvik, G.E., Butenko, M.A., Kristiansen, W., Cho, S. K., Hepworth, S.R., Aalen, R.B., and Haughn, G.W.** (2008). The BLADE-ON-PETIOLE genes are essential for abscission zone formation in Arabidopsis. *Development* **135**: 1537–1546.
- McMullen, C.R., Gardner, W.S., and Myers, G.A.** (1977). Ultrastructure of cell-wall thickenings and paramural bodies induced by barley stripe mosaic virus. *Phytopathology* **67**: 462–467.
- Meir, S., Hunter, D.A., Chen, J.C., Halaly, V., and Reid, M.S.** (2006). Molecular changes occurring during acquisition of abscission competence following auxin depletion in *Mirabilis jalapa*. *Plant Physiol.* **141**: 1604–1616.
- Meir, S., Philosoph-Hadas, S., Sundaresan, S., Selvaraj, K.S., Burd, S., Ophir, R., Kochanek, B., Reid, M.S., Jiang, C.-Z., and Lers, A.** (2010). Microarray analysis of the abscission-related transcriptome in the tomato flower abscission zone in response to auxin depletion. *Plant Physiol.* **154**: 1929–1956.
- Niu, Y., Chen, K.L., Wang, J.Z., Liu, X., Qin, H.J., Zhang, A.M., and Wang, D.W.** (2007). Molecular and functional characterization of sphingosine-1-phosphate lyase homolog from higher plants. *J. Integr. Plant Biol.* **49**: 323–335.
- Ogawa, M., Kay, P., Wilson, S., and Swain, S.M.** (2009). ARABIDOPSIS DEHISCENCE ZONE POLYGALACTURONASE1 (ADPG1), ADPG2, and QUARTET2 are polygalacturonases required for cell separation during reproductive development in *Arabidopsis*. *Plant Cell* **21**: 216–233.
- Orzaez, D., de Jong, A.J., and Woltering, E.J.** (2001). A tomato homologue of the human protein PIRIN is induced during programmed cell death. *Plant Mol. Biol.* **46**: 459–468.
- Osborne, D.J., and Sargent, J.A.** (1976). The positional differentiation of abscission zones during the development of leaves of *Sambucus nigra* and the response of the cells to auxin and ethylene. *Planta* **132**: 197–204.
- Oskouian, B., Sooriyakumaran, P., Borowsky, A.D., Crans, A., Dillard-Telm, L., Tam, Y.Y., Bandhuvula, P., and Saba, J.D.** (2006). Sphingosine-1-phosphate lyase potentiates apoptosis via p53- and p38-dependent pathways and is down-regulated in colon cancer. *Proc. Natl. Acad. Sci. USA* **103**: 17384–17389.
- Patterson, S.E.** (2001). Cutting loose. Abscission and dehiscence in *Arabidopsis*. *Plant Physiol.* **126**: 494–500.
- Reape, T.J., and McCabe, P.F.** (2010). Apoptotic-like regulation of programmed cell death in plants. *Apoptosis* **15**: 249–256.
- Reiss, U., Oskouian, B., Zhou, J.H., Gupta, V., Sooriyakumaran, P., Kelly, S., Wang, E., Merrill, A.H., Jr., and Saba, J.D.** (2004). Sphingosine-phosphate lyase enhances stress-induced ceramide generation and apoptosis. *J. Biol. Chem.* **279**: 1281–1290.

- Roberts, J.A.** (2000). Abscission and dehiscence. In *Programmed Cell Death in Animals and Plants*, J.A. Bryant, S.G. Hughes, and J.M. Garland, eds (Oxford, UK: BIOS Scientific Publishers), pp. 203–211.
- Roberts, J.A., Elliott, K.A., and González-Carranza, Z.H.** (2002). Abscission, dehiscence, and other cell separation processes. *Annu. Rev. Plant Biol.* **53**: 131–158.
- Roberts, J.A., Schindler, C.B., and Tucker, G.A.** (1984). Ethylene-promoted tomato flower abscission and the possible involvement of an inhibitor. *Planta* **160**: 159–163.
- Roberts, J.A., Whitelaw, C.A., González-Carranza, Z.H., and McManus, M.T.** (2000). Cell separation processes in plants - Models, mechanisms and manipulation. *Ann. Bot. (Lond.)* **86**: 223–235.
- Sakamoto, M., Munemura, I., Tomita, R., and Kobayashi, K.** (2008). Involvement of hydrogen peroxide in leaf abscission signaling, revealed by analysis with an *in vitro* abscission system in *Capsicum* plants. *Plant J.* **56**: 13–27.
- Sexton, R., and Roberts, J.A.** (1982). Cell biology of abscission. *Annu. Rev. Plant Physiol. Plant Mol. Biol.* **33**: 133–162.
- Shani, Z., Dekel, M., Roiz, L., Horowitz, M., Kolosovski, N., Lapidot, S., Alkan, S., Koltai, H., Tsabary, G., Goren, R., and Shoseyov, O.** (2006). Expression of endo-1,4-beta-glucanase (*cel1*) in *Arabidopsis thaliana* is associated with plant growth, xylem development and cell wall thickening. *Plant Cell Rep.* **25**: 1067–1074.
- Sparvoli, F., Faoro, F., Daminati, M.G., Ceriotti, A., and Bollini, R.** (2000). Misfolding and aggregation of vacuolar glycoproteins in plant cells. *Plant J.* **24**: 825–836.
- Stenvik, G.E., Tandstad, N.M., Guo, Y., Shi, C.L., Kristiansen, W., Holmgren, A., Clark, S.E., Aalen, R.B., and Butenko, M.A.** (2008). The EPIP peptide of INFLORESCENCE DEFICIENT IN ABSCISSION is sufficient to induce abscission in *Arabidopsis* through the receptor-like kinases HAESA and HAESA-LIKE2. *Plant Cell* **20**: 1805–1817.
- Taylor, J.E., and Whitelaw, C.A.** (2001). Signals in abscission. *New Phytol.* **151**: 323–339.
- Tirlapur, U.K., Costa, G., Malossini, C., Vizzotto, G., and Cresti, M.** (1995). Scanning electron microscopy, video-image analysis, and confocal imaging of changes occurring during peach fruit abscission. *J. Am. Soc. Hortic. Sci.* **120**: 203–210.
- Torres, M.A., and Dangl, J.L.** (2005). Functions of the respiratory burst oxidase in biotic interactions, abiotic stress and development. *Curr. Opin. Plant Biol.* **8**: 397–403.
- Torres, M.A., Dangl, J.L., and Jones, J.D.G.** (2002). *Arabidopsis gp91phox* homologues *AtrbohD* and *AtrbohF* are required for accumulation of reactive oxygen intermediates in the plant defense response. *Proc. Natl. Acad. Sci. USA* **99**: 517–522.
- Tripathi, S.K., Singh, A.P., Sane, A.P., and Nath, P.** (2009). Transcriptional activation of a 37 kDa ethylene responsive cysteine protease gene, *RbCP1*, is associated with protein degradation during petal abscission in rose. *J. Exp. Bot.* **60**: 2035–2044.
- Trobacher, C.P.** (2009). Ethylene and programmed cell death in plants. *Botany* **87**: 757–769.
- Tucker, G.A., Schindler, C.B., and Roberts, J.A.** (1984). Flower abscission in mutant tomato plants. *Planta* **160**: 164–167.
- Van Breusegem, F., and Dat, J.F.** (2006). Reactive oxygen species in plant cell death. *Plant Physiol.* **141**: 384–390.
- van Doorn, W.G., et al.** (2011). Morphological classification of plant cell deaths. *Cell Death Differ.* **18**: 1241–1246.
- van Doorn, W.G., and Stead, A.D.** (1997). Abscission of flowers and floral parts. *J. Exp. Bot.* **48**: 821–837.
- van Nocker, S.** (2009). Development of the abscission zone. *Stewart Postharvest Rev.* **5**: 1–6.
- Vanyushin, B.F., Bakeeva, L.E., Zamyatnina, V.A., and Aleksandrushkina, N.I.** (2004). Apoptosis in plants: Specific features of plant apoptotic cells and effect of various factors and agents. *Int. Rev. Cytol.* **233**: 135–179.
- Wang, Y.C., Li, T.L., Meng, H.Y., and Sun, X.Y.** (2005). Optimal and spatial analysis of hormones, degrading enzymes and isozyme profiles in tomato pedicel explants during ethylene-induced abscission. *Plant Growth Regul.* **46**: 97–107.
- Wang, Z.H., Song, J.H., Zhang, Y., Yang, B.Y., and Chen, S.Y.** (2009). Expression of baculovirus anti-apoptotic *p35* gene in tobacco enhances tolerance to abiotic stress. *Biotechnol. Lett.* **31**: 585–589.
- Webster, B.D.** (1973). Ultrastructural studies of abscission in *Phaseolus*: Ethylene effects on cell walls. *Am. J. Bot.* **60**: 436–447.
- Wijayanto, T., Barker, S.J., Wylie, S.J., Gilchrist, D.G., and Cowling, W.A.** (2009). Significant reduction of fungal disease symptoms in transgenic lupin (*Lupinus angustifolius*) expressing the anti-apoptotic baculovirus gene *p35*. *Plant Biotechnol. J.* **7**: 778–790.
- Woltering, E.J.** (2010). Death proteases: Alive and kicking. *Trends Plant Sci.* **15**: 185–188.
- Yang, Y.L., and Li, X.M.** (2000). The IAP family: Endogenous caspase inhibitors with multiple biological activities. *Cell Res.* **10**: 169–177.